Geophysical Journal International

Geophys. J. Int. (2011) **184,** 555–574 doi: 10.1111/j.1365-246X.2010.04874.x

Right-lateral shear across Iran and kinematic change in the Arabia–Eurasia collision zone

Mark B. Allen,[1,*] Monireh Kheirkhah,[2] Mohammad H. Emami[2] and Stuart J. Jones[1]

[1]*Department of Earth Sciences, University of Durham, Durham, DH1 3LE, UK. E-mail: m.b.allen@durham.ac.uk*
[2]*Research Institute for Earth Sciences, Geological Survey of Iran, Azadi Square, Meraj Avenue, Tehran, Iran*

Accepted 2010 October 29. Received 2010 October 07; in original form 2010 April 7

SUMMARY

New offset determinations for right-lateral strike-slip faults in Iran revise the kinematics of the Arabia–Eurasia collision, by indicating along-strike lengthening of the collision zone before a change to the present kinematic regime at ∼5 Ma. A series of right-lateral strike-slip faults is present across the Turkish–Iranian plateau between 48°E and 57°E. Fault strikes vary between NW–SE and NNW–SSE. Several of the faults are seismically active and/or have geomorphic evidence for Holocene slip. None of the faults affects the GPS-derived regional velocity field, indicating active slip rates are ≤2 mm yr^{-1}. We estimate total offsets for these faults from displaced geological and geomorphic markers, based on observations from satellite imagery, digital topography, geology maps and our own fieldwork observations, and combine these results with published estimates for fault displacement. Total right-lateral offset of the Dehu, Anar, Deh Shir, Kashan, Ab-Shirin-Shurab, Kousht Nousrat, Qom, Bid Hand, Indes, Soltanieh and Takab faults is ∼250 km. Other faults (North Zanjan, Saveh, Jorjafk, Rafsanjan, Kuh Banan and Behabad) have unknown or highly uncertain amounts of slip. Collectively, these faults are inferred to have accommodated part of the Arabia–Eurasia convergence. Three roles are possible, which are not mutually exclusive: (1) shortening via anticlockwise, vertical axis rotations; (2) northward movement of Iranian crust with respect to stable Afghanistan to the east; (3) combination with coeval NW–SE thrusts in the Turkish–Iranian plateau, to produce north–south plate convergence ('strain partitioning'). This strike-slip faulting across Iran requires along-strike lengthening of the collision zone. This was possible until the Pliocene (≤ 5 Ma), when the Afghan crust collided with the western margin of the Indian plate, thereby sealing off a free face at the eastern side of the Arabia–Eurasia collision zone. Continuing Arabia–Eurasia plate convergence had to be accommodated in new ways and new areas, leading to the present pattern of faulting from eastern Iran to western Turkey, and involving the westward transport ('escape') of Anatolia and the concentration of thrusting in the Zagros and Alborz mountains.

Key words: Continental neotectonics; Continental tectonics: strike-slip and transform; Tectonics and landscape evolution; Asia.

1 INTRODUCTION

This paper describes the offset and ages of a series of right-lateral strike-slip faults across Iran, and interprets this deformation in the context of the Arabia–Eurasia collision zone. The faults have a general NW–SE or NNW–SSE trend and occur between 48ºE and 57ºE (Fig. 1a). At these longitudes nearly all of the plate convergence occurs within Iran, making a relatively compact study area for continental tectonics.

Present day kinematics of the collision zone are broadly understood through combinations of seismicity and GPS studies (Fig. 2; Jackson *et al*. 1995; Vernant *et al*. 2004). Active thickening (thrusting) in Iran takes place at the north and south sides of the collision, in the Alborz, Kopeh Dagh and Zagros mountains (Allen *et al*. 2003; McQuarrie 2004; Talebian & Jackson 2004; Hollingsworth *et al*. 2010). Much of Turkey moves westwards between the North and East Anatolian faults, in the classic example of escape tectonics (McKenzie 1972). Thrusting takes place in the Greater Caucasus (Philip *et al*. 1989). Strike-slip faults form a sharp western boundary (Dead Sea Fault System; Garfunkel 1981) and diffuse eastern boundary (eastern Iran) to the deforming zone (Walker & Jackson 2004; Meyer *et al*. 2006). Active subduction occurs to the west and east of the collision, in the Aegean and Makran regions (Reilinger *et al*. 2006). The South Caspian basement moves westwards with

*Correction made after online publication 2011 January 17: the affiliation number for the first author is now correct.

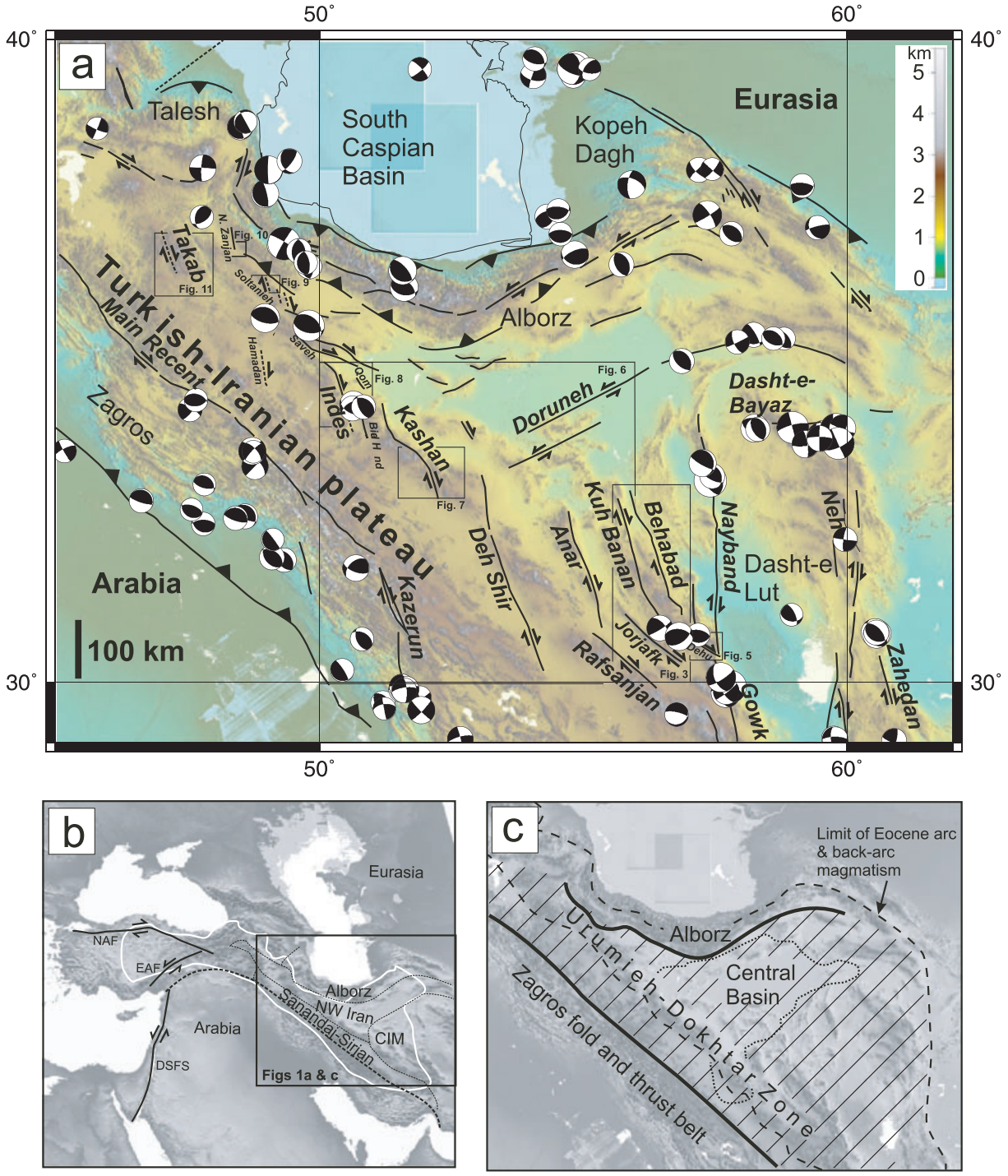

Figure 1. (a) Regional structure and seismicity, highlighting the active fault systems of Iran and adjacent areas. Dashed lines indicate strike-slip faults within this study that are not necessarily active. Focal mechanisms are from Jackson (2001) for earthquakes between 1959 and 2000 August 22 (determined by body-wave analysis) and from the Harvard catalogue (http://www.globalcmt.org/) for later events upto 2008 March 31. The routinely determined catalogue records are filtered for $M_w > 5$ and > 70 per cent double-couple solutions. (b) Location map for (a). Thick white line is the approximate boundary of the Turkish–Iranian plateau. Dashed lines mark basement block boundaries within Iran. CIM, Central Iranian Microcontinent; DSFS, Dead Sea Fault System; EAF, East Anatolian Fault; NAF, North Anatolian Fault. (c) Cenozoic tectonic units of Iran. The extent of Central Iran is shown by hatching between the Zagros suture and the southern side of the Alborz (solid lines).

respect to stable Eurasia as a relatively rigid block, with strike-slip to its south (Alborz) and northeast (Kopeh Dagh) (Jackson *et al*. 2002; Ritz *et al*. 2006).

Less is known about earlier patterns of deformation, how plate convergence was achieved on faults that are now inactive, and when, how and why the transition to the current pattern of faulting took place. Initial collision timing is an important baseline for understanding long-term deformation patterns. This has been the subject of much debate over the years, with common estimates including the Late Eocene (~37–34 Ma) (e.g. Allen & Armstrong 2008; Ballato

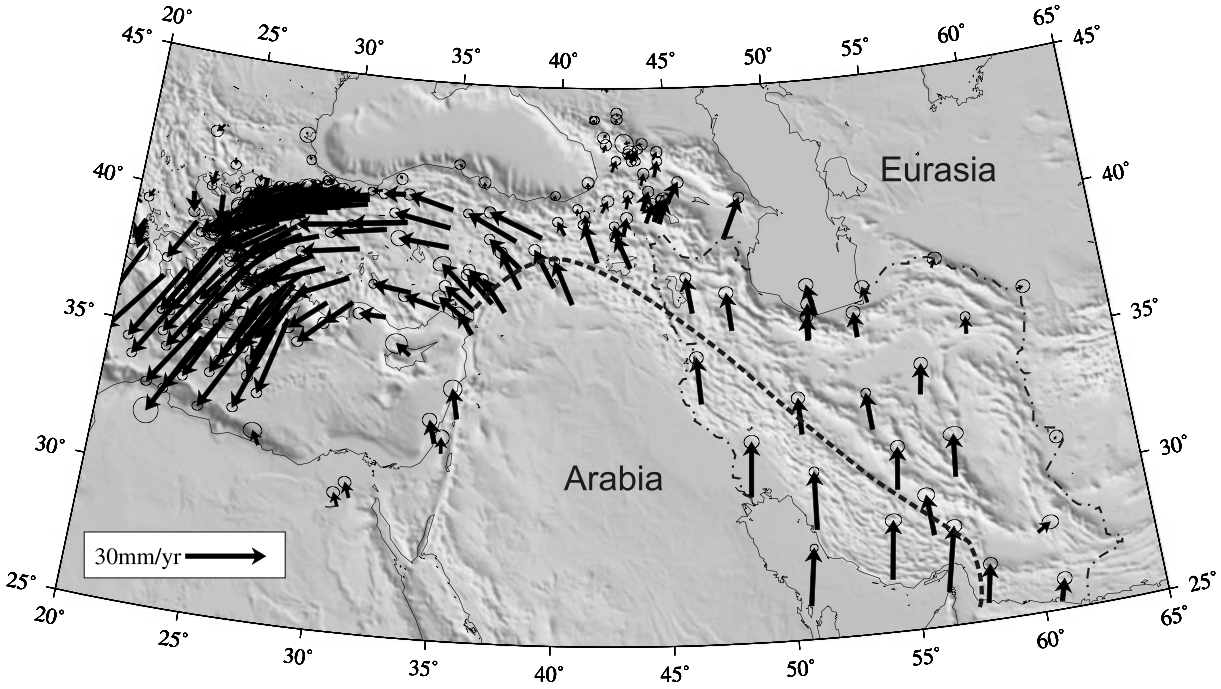

Figure 2. GPS-derived velocity field for the Arabia–Eurasia collision, with respect to a stable Eurasia reference frame (McClusky *et al.* 2000; Vernant *et al.* 2004). Thick dashed line shows approximate Arabia–Eurasia suture. Iran national border highlighted.

et al. 2010) and Early Miocene (∼20 Ma) (e.g. Okay *et al*. 2010). The active tectonic pattern cannot simply be extrapolated back to the initial collision, whichever estimate of ≥20 Ma is correct, for two reasons. The first is that present slip rates on several of the major active faults need only be extrapolated for ≤10 Ma before they account for the total deformation on these structures. Examples include strike-slip faults such as the North and East Anatolian faults, the north–south right-lateral faults in easternmost Iran, the right-lateral Lesser Caucasus faults (Westaway 1994; McClusky *et al*. 2000; Vernant *et al*. 2004; Walker & Jackson 2004; Copley & Jackson 2006). Thrust belts include the Zagros Simple Folded Zone, the Alborz and the Kopeh Dagh (Berberian 1995; Blanc *et al*. 2003; Guest *et al*. 2006; Hollingsworth *et al*. 2008).

A second reason is that there are regions within the collision zone that show evidence for late Cenozoic compressional deformation (so post-dating the initial collision) but are inactive, or at least not thrusting at present. Large parts of the Turkish–Iranian plateau fall in to this category. The plateau has an area of 1500 000 km^2 and typical elevations of 1.5–2 km—declining to ∼500 m in eastern Iran. In Iran, basement consists largely of Gondwana-derived microcontinents: the Sanandaj-Sirjan Zone, NW Iran and the Central Iranian Microcontinent (Fig. 1b). There is little seismicity evidence for active thrusting (except localized at the ends of strike-slip faults), and GPS data show that shortening rates across the Turkish–Iranian plateau, between the Alborz and Zagros mountains, are only ∼2 mm yr^{-1} at the most (Vernant *et al*. 2004). Active strike-slip faults deform parts of the plateau, especially in eastern Anatolia and NW Iran west of 48°E, with ∼NE–SW trending left-lateral and ∼NW–SE trending right-lateral faults. The latter faults rotate anticlockwise about vertical axes, to achieve greater NNE–SSW shortening across the eastern part of the Caucasus than further west (Copley & Jackson 2006). Cenozoic crustal thickening is evident from folded and thrusted strata (National Iranian Oil Company (NIOC) 1977a, 1977b, 1978; Fattahi *et al*. 2006; Morley *et al*. 2009), although not many details are known at present.

We use the expression 'Central Iran' for that part of the plateau northeast of the Zagros suture and south of the Alborz mountains. Central Iran therefore includes the Sanandaj-Sirjan Zone and the NW Iran and Central Iran microcontinents (Fig. 1b). These basement blocks are overlain by the Urumieh-Dokhtar Zone (an early Cenozoic, predominantly Eocene, magmatic arc), and to its northeast, the Central Basin (Fig. 1c; Morley *et al*. 2009). Extensive Eocene volcanics underlie the Central Basin and are exposed within large parts of the Alborz to its north (Vincent *et al*. 2005). In contrast, the Urumieh-Dokhtar Zone has a linear, NW–SE volcanic front along its southwestern side. Central Iran is therefore geologically distinct from regions to the southwest that also lack thrust seismicity and active shortening and thickening, but are geologically part of the Zagros, and belong to the Arabian plate.

It seems that the Turkish–Iranian plateau has absorbed part of the Arabia–Eurasia convergence by crustal shortening and thickening, but it does not do so now, given the GPS and seismicity data. Allen *et al*. (2004) suggested that thrusting has migrated towards the present margins of the collision zone, in the lower elevation parts of the Zagros and the borders of the South Caspian Basin, once the Turkish–Iranian plateau achieved enough elevation for a buoyancy force to resist further shortening. This could be achieved by crustal thickening, dynamic mantle support (Maggi & Priestley 2005) or some combination of the two (Copley & Jackson 2006).

This paper aims to improve our understanding of the Cenozoic deformation of the Turkish–Iranian plateau, and so the large-scale patterns of continental deformation within the Arabia–Eurasia collision as a whole. Although we do not conduct a specific seismic hazard study, our results bear on the issue. In the next part of the paper we use satellite imagery, geological maps, digital topography (SRTM), fieldwork and the literature to constrain the offset on strike-slip faults within the Iranian part of the Turkish–Iranian plateau. We then use these data to try and understand why this slip occurred, with three identified roles: (1) ∼north–south shortening associated with fault block rotation about vertical axes; (2) motion

of crust northwards with respect to blocks further east and (3) combination with coeval thrusting and folding, assuming that oblique convergence is split ('partitioned') in to dip-slip and strike-slip components. Roles (1) and (2) have been suggested before for some of the faults in this study (Walker & Jackson 2004; Meyer *et al*. 2006). We finally ask why deformation appears to have stopped or slowed in the last few million years on most of the studied faults, and develop a kinematic model based on a boundary condition change to the east of the collision zone. This model, based on a Pliocene age for the collision between India and the Afghan crust (Treloar & Izatt 1993), is speculative, but has implications for Late Cenozoic tectonic reorganization across SW Asia.

2 RIGHT-LATERAL FAULTS

Following parts of this section describe right-lateral strike-slip faults within the Iranian sector of the Turkish–Iranian plateau, from 48° to 57°E (Fig. 1). This is an area with a modest historical and instrumental seismicity record compared with adjacent regions in the Zagros and Alborz mountains (Berberian & Yeats 1999). There is little internal deformation detected in currently available, GPS-derived velocity fields (Fig. 2; Vernant *et al*. 2004). At the eastern end of the study area, the Anar and Deh Shir faults (Fig. 1) have offset presumed early Holocene sediments, with slip rates estimated as ∼1–2 mm yr^{-1} (Meyer *et al*. 2006; Meyer and Le Dortz 2007; Le Dortz *et al*. 2009). The Kuh Banan Fault experienced $M_w > 5$ earthquakes in 1979 and 2005 (Talebian *et al*. 2006). There is strong seismicity on the north–south trending Nayband-Gowk system, at the eastern margin of the study area (Walker *et al*. 2009), representing part of the north–south shear at the eastern side of the collision zone as a whole. Three earthquakes of magnitude >5 are recorded near the Bid Hand Fault (Fig. 1), but other faults lack instrumental seismicity on this scale.

For each fault we use available geological and geomorphological data to describe the nature of the fault (especially its total slip), constraints on the timing of deformation and evidence (if any) for Holocene activity. We use the results in Section 3 to examine how the right-lateral slip could have contributed to overall north–south plate convergence. Some of the fault histories may relate to pre-collision tectonics within Eurasia, but this is not a significant factor, because offset geological markers are typically Eocene or younger, that is, post-dating or only just pre-dating initial collision. However, Fig. 1(a) includes the location of the right-lateral ductile NNW–SSE shearing identified by Agard *et al*. (2005) east of the Alvand pluton, Hamadan, which is loosely constrained to be early Tertiary in age. Faults are described from east to west; this is generally the direction in which fault length and verifiable offset decreases. Some faults are discussed in a single section where they are close to each other.

Table 1 summarises the offset estimates for the individual faults: the combined total is ∼250 km, not including the Behabad, Kuh Banan, Jorjafk, Rafsanjan, Saveh and North Zanjan faults (Fig. 1) for which we have no estimates.

2.1 Kuh Banan, Dehu and Behabad Faults

The Kuh Banan Fault is ∼280 km long and trends ∼NNW–SSE, which is parallel to the strike-slip faults to its east and west (Figs 1 and 3). Along strike from northwest to southeast the main fault switches from being on the east side of the range to the west (Fig. 3). Two topographic depressions at right-lateral jogs along the fault may be pull-apart basins. The fault is more segmented in the north, with several sub-parallel strands (Mahdavi 1996). Its total strike-slip offset is not known. The ∼1 km of topographic relief across the fault indicates a component of thrust slip directed from southwest to northeast in the north, and northeast to southwest in the south, but the amount is not known.

The Kuh Banan Fault is seismically active (Berberian *et al*. 1979; Talebian *et al*. 2006). An earthquake on 1977 December 19 (main shock epicentre 30.9°N 56.6°E; M_s 5.8) caused a 19.5 km long surface break associated with 20 cm of right-lateral slip (Fig. 3). The fault plane solution is a right-lateral event, with the preferred nodal plane striking N148°E and dipping at 58° towards the northeast (Berberian *et al*. 1979). Other events occurred along the northern part of the fault in 1933 and 1978 (Fig. 3). The fault has sections that variously cut across alluvium, juxtapose bedrock and alluvium or juxtapose different units of bedrock. At roughly 30.7°N 56.8°E the Kuh Banan Fault becomes less distinct and WNW–ESE trending thrusts become prominent (Fig. 3). One of these thrust faults (Dahuiyeh) ruptured in 2005 (Talebian *et al*. 2006).

Numerous streams and rivers show evidence for right-lateral offset along the southern segment of the Kuh Banan Fault. Offset is variable, ranging from 10 to 20 m for minor streams to hundreds of metres for larger drainages. The largest rivers have ∼1 km of offset. Figs 4(a)–(c) show examples of these right-lateral offsets at different length scales, including examples where multiple stream offsets can be restored. The ages of these offset features are not known. There are estimates for the age of the change from alluvial fan aggradation to incision elsewhere in eastern Iran (Fattahi *et al*. 2006; Regard *et al*. 2006; Fattahi *et al*. 2007), which suggest regional climatic change in the early Holocene at ∼12 ± 2 ka (see also Meyer & Le Dortz 2007). This is a possible but far from certain age for the youngest channels offset along the Kuh Banan Fault and other faults in this study. If true, it implies the Holocene slip rate on the Kuh Banan Fault is 1–2 mm yr^{-1}. The rate is obviously higher if the features are younger, as deduced for the latest offset features on the Anar Fault (Le Dortz *et al*. 2009).

Roughly where the Kuh Banan Fault becomes less visible in the geology and geomorphology, the NW–SE trending Dehu Fault begins (Figs 3 and 5; Sahandi 1992), connected by the WNW–ESE trending thrusts in the Dahuiyeh area. Right-lateral offset of up to ∼20 km is discernible on the Dehu Fault, where folded Precambrian-Paleogene strata are offset (Fig. 5). The youngest strata deformed in the offset folds are the Paleocene-Eocene Kerman Conglomerates, suggesting that initial strike-slip movement post-dates this time. Diapirs of Precambrian gypsum complicate the structure, as does a NE–SW trending left-lateral fault that intersects the Dehu Fault. Two possible piercing points on the Dehu Fault are picked out in Fig. 5. These are not definitive and the offset needs further study. A syncline with Middle Jurassic strata in its core can possibly be matched across the Dehu Fault near Horjond, with an offset of ∼20 km. This is the only syncline involving strata of this age to be offset, and it is at a high angle to the fault, which gives confidence that the offset is real and not an artefact of dip-slip displacement of a feature at a low angle to the fault. Another plausible right-lateral offset occurs at a locality 15 km to the southeast, where a WNW–ESE trending syncline, cored by Cretaceous-Paleogene strata, is displaced for 2–3 km (Fig. 5), noted by Walker *et al*. (2010). A strike-slip component to the fault displacement is supported by the sub-vertical dip of the fault at exposed levels (Sahandi 1992) and the changing age relationships across it: older rocks are present on the southwest side of the fault in the northwest, whereas in the southeast the older rocks are on the northeast side. These relationships are not compatible with a simple dip-slip structure, but make sense

Table 1. Summary of right-lateral strike-slip faults across Central Iran.

Fault name	Total offset, km (previous work)	Total offset, km (this study)	Instrumental seismicity ($M \geq 5$)	Historical seismicity ($M \geq 5$)	Geomorphic Holocene activity	Active slip rate (mm yr^{-1})	References
Dehu	2–3	20	No	Yes	Yes	?	Sahandi (1992), Walker *et al*. (2010)
Kuh Banan		?	Yes	Yes	Yes	1.5 – poorly constrained	Berberian *et al*. (1979), Talebian *et al*. (2006)
Behabad		?	No	Yes	Probably	1.5 – poorly constrained	Berberian *et al*. (1979), Mahdavi (1996)
Jorjafk		?	No	No	Yes	<1 – poorly constrained	Berberian & Yeats (1999), Vahdati Daneshmand (1992), Walker *et al*. (2010)
Rafsanjan		?	No	Yes	Yes	?	Vahdati Daneshmand (1992), Walker (2006), Walker *et al*. (2010)
Anar	25 ± 5		No	Yes	Yes	≥0.8	Walker & Jackson (2004), Meyer & Le Dortz (2007), Le Dortz *et al*. (2009)
Deh Shir	65 ± 15		No	No	Yes	∼2	Walker & Jackson (2004), Meyer *et al*. (2006)
Kashan		40	No	Yes	Yes	≥2	NIOC (1977a), Jamali *et al*. (2010)
Ab-Shirin-Shurab	4		No	Yes	?	?	Morley *et al*. (2009)
Bid Hand		≤ 2	Yes	Yes	?	?	Emami (1981)
Qom		5	No	No	?	?	Zamani-pedram & Hossaini (1998)
Saveh		?	No	Yes	?	?	Morley *et al*. (2009)
Koushk-Nousrat	9 ± 2		No	Yes	?	?	Morley *et al*. (2009)
Indes		50	No	Yes	?	?	Emami (1981), Morley *et al*. (2009)
Soltanieh		15	No	No	No	0	Stöcklin & Eftekharnezhad (1969); Berberian (1976)
North Zanjan		?	No	No	Yes	?	Stöcklin & Eftekharnezhad (1969), NIOC (1978)
Takab		15	No	Yes	No	0	Alavi & Amidi (1976), Daliran (2008)

if a folded region is cut by a strike-slip fault, possibly with a helicoidal form, that is, changing in dip direction along its length. There are no major (magnitude >5) instrumentally recorded earthquakes along the Dehu Fault (Fig. 1), but there were three 19th century events on this scale (Ambraseys & Melville 1982; Fig. 5). Walker *et al*. (2010) noted scarps in late Quaternary alluvial fans, along the trace of a NW–SE fault between the Dehu and Dehran faults (Fig. 5).

Little is known about the Behabad (Ravar) Fault, mapped by Mahdavi (1996) as a right-lateral strike-slip fault to the northeast of the Kuh Banan Fault (Fig. 3). The northern part of the fault trends NNW–SSE, but it changes to a NW–SE orientation at the range front close to the town of Ravar (31.25°N 56.8°E). We interpret this left-stepping jog in the fault as a segment with thrust slip at a restraining bend. The continuation south of this jog is not clear, but it may link via disjointed segments into the folded and thrusted region adjacent to the Kuh Banan Fault. The total offset of the Behabad Fault is not known. Destructive earthquakes took place in 1903 and 1913 close to the Behabad Fault, south of Ravar (Fig. 3; Berberian *et al*. 1979), with the latter event causing surface rupture. Three earthquakes occurred within 25 km of the fault trace, but further south of Ravar, in 1913, 1953 and 1959 (Fig. 3); it is not clear if these events related to slip on the Behabad Fault itself or other structures in the vicinity. Four other 20th century earthquakes occurred near the northern trace of the fault (Berberian *et al*. 1979). Displaced alluvial fans along the northern part of the fault indicate Quaternary and possibly Holocene slip. A possible right-lateral offset of a river channel edge of 18 m is shown in Fig. 4(d). The age of this feature is not known. If it is early Holocene, as discussed above for the youngest offset channels along the Kuh Banan Fault, this corresponds to a slip rate of ∼1.5 mm yr^{-1}.

2.2 Jorjafk and Rafsanjan Faults

The Kuh-e Daviran range runs for ∼180 km between the Rafsanjan and Kuh Banan faults (Fig. 3). The range is bounded for most of its length along its northeast side by the linear NW–SE Jorjafk Fault, which separates it from alluvial plains further to the northeast (Vahdati Daneshmand 1992; Berberian & Yeats 1999; Walker *et al*. 2010). For much of the fault length there is a prominent, linear topographic break between the bedrock and alluvium, and up to ∼1 km topographic relief between the crest of the Kuh-e Daviran range and the lowlands to the northeast (Fig. 3). This relief implies a component of thrust slip, southwest to northeast over the adjacent plain. In the southeast of the range there is no sharply defined, range-bounding fault, but en echelon faults cut obliquely across the range interior. The bedrock geology in the Kuh-e Daviran range is complex, making slip restoration estimates for the Jorjafk Fault harder than for some parts of the plateau.

For 15 km the fault cuts across alluvium, with a possible right-lateral offset of a river channel by ∼15 m at 30.83° N 56.08° E (Fig. 4e). The age of this channel is not known. Assuming an age of 12 ± 2 ka for the channel in Fig. 4(e), as argued above for similar features along the Kuh Banan and Behabad faults, yields a slip rate of <1 mm yr^{-1} on the Jorjafk Fault, which seems feasible.

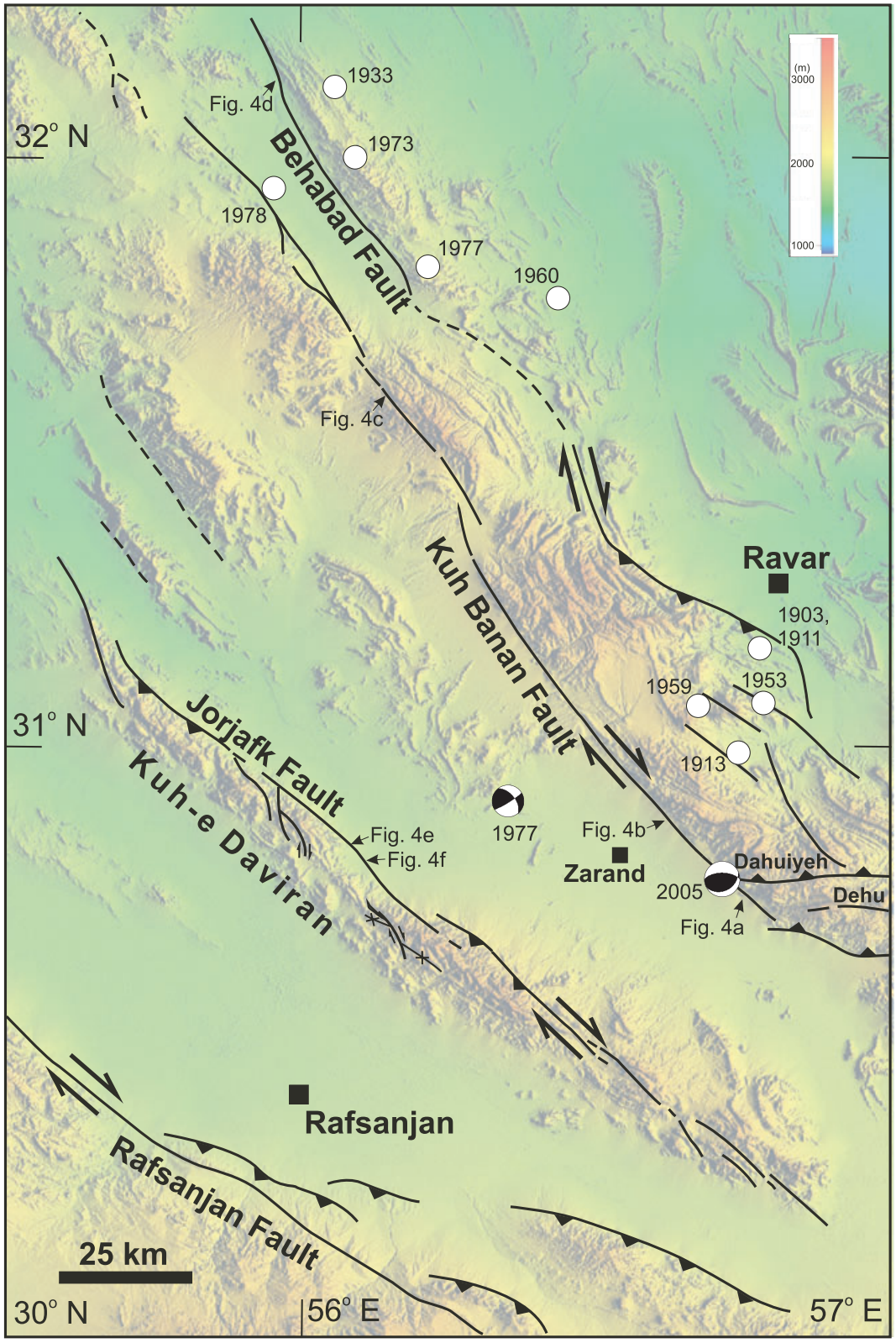

Figure 3. Active fault map of the Rafsanjan region overlain on shaded relief SRTM imagery. Right-lateral strike-slip faults predominate (Rafsanjan, Jorjafk, Kuh Banan and Behabad), with some component of thrusting shown by the topographic and structural relief between mountainous areas and adjacent plains. Earthquake focal mechanisms are from Baker (1993) and Talebian *et al.* (2006) for the 1977 and 2005 events, respectively. Historical events are from Ambraseys & Melville (1982) and Berberian *et al*. (1979).

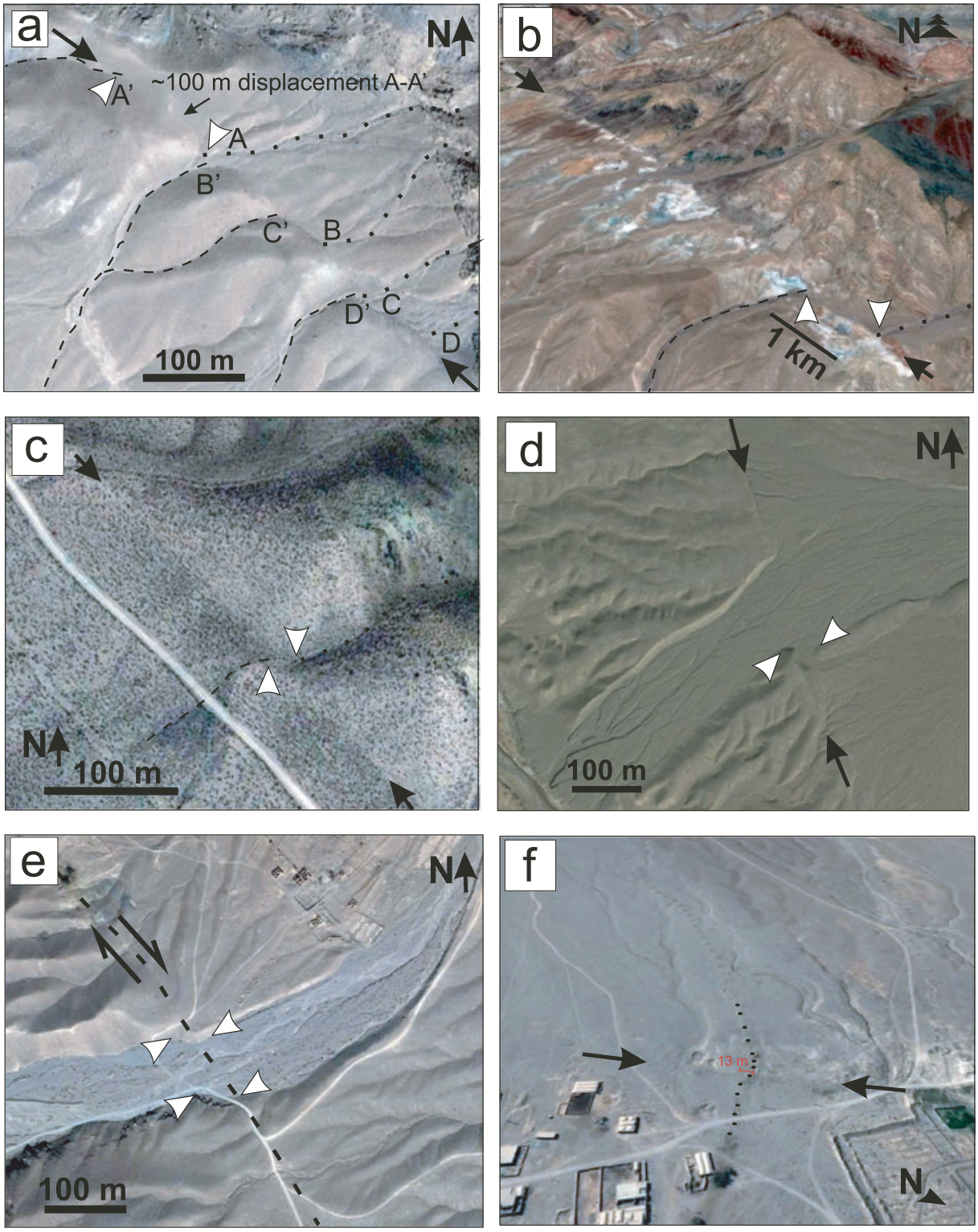

Figure 4. Quickbird satellite imagery (from Google Earth, ©2010 Google, ©2010 DigitalGlobe) shows active slip along the Kuh Banan, Behabad and Jorjafk faults. (a) The Kuh Banan Fault (arrowed) cuts alluvial fans 500 m east of Asghar village. Streams are displaced right-laterally by ∼100–140 m, correlating streams A–D with A′–D′ on the downstream side of the fault. The restoration brings stream A into line with the beheaded stream A′ and removes the current jog in the downstream course of stream B. (b) Oblique view of the Kuh Banan Fault 10 km northeast of Zarand, showing a river displaced right-laterally by ∼1 km (white arrows) where it crosses the fault trace (black arrows). Light patches along the fault are evapourites, mapped as Precambrian in age. There is no vertical exaggeration. (c) The Kuh Banan Fault (black arrows) offsets a stream gully by ∼14 m (white arrows). Location: 31.58° N 56.15° E. (d) A possible ∼18 m offset of a river channel bank (white arrows) along the Behabad Fault (black arrows). Location: 32.15° N 55.95° E. (e) The Jorjafk Fault apparently displaces a river channel bank by ∼15 m (white arrows), 45 km west of Zarand. (f) Oblique view of a locality 45 km west of Zarand where the trend of a qanat jogs right-laterally by 13 m across the Jorjafk Fault trace (arrowed). Locations shown on Fig. 3.

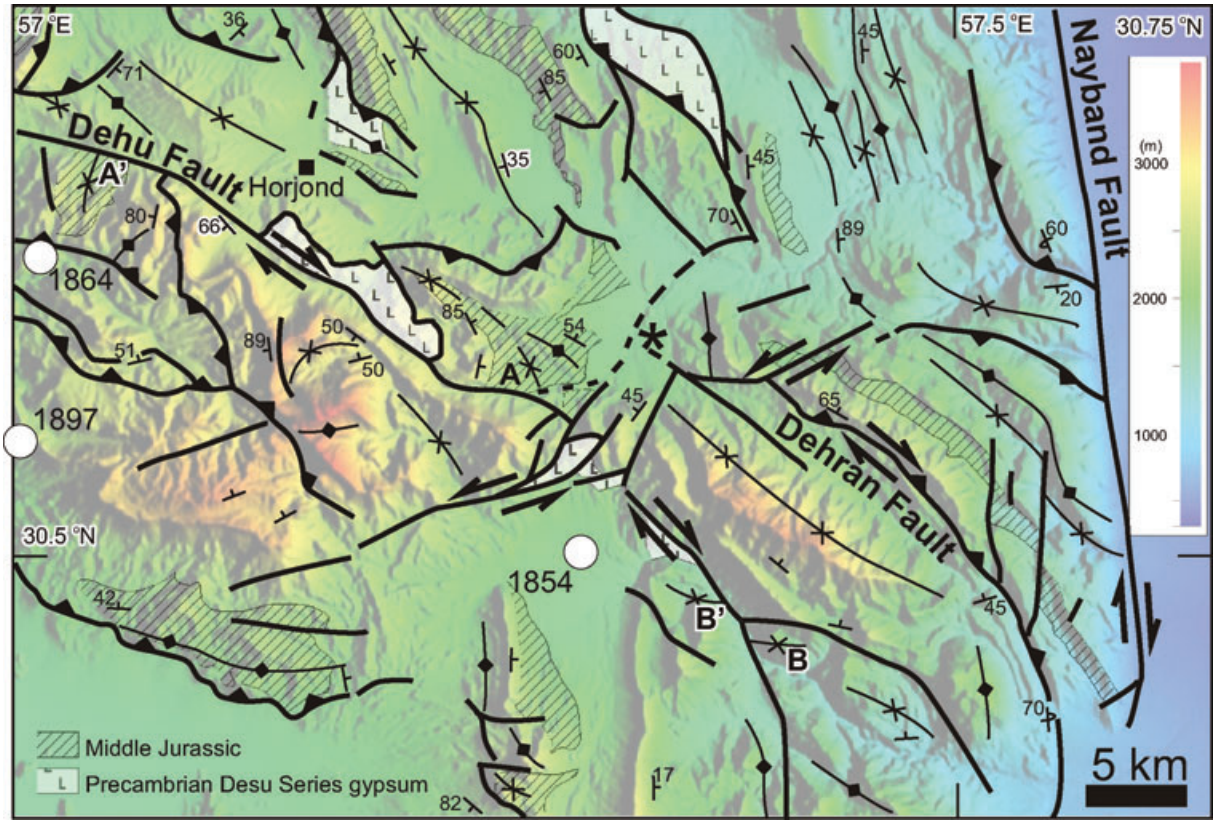

Figure 5. Faults, folds and selected formations in the Horjond region overlain on shaded-relief SRTM imagery, illustrating the right-lateral offset of geological markers on either side of the Dehu Fault (geology from Sahandi 1992). Middle Jurassic strata in a syncline are offset between points A and A′ by ∼20 km. Points B–B′ show a much smaller offset folded Cretaceous strata, of 2–3 km, further southeast along the fault (Walker *et al*. 2010). Extrusions of Precambrian gypsum complicate the regional geology. No instrumentally recorded earthquakes with $M_w > 5$ are recorded from this region. The asterisk symbol marks the locations of NW–SE scarps in late Quaternary alluvial fans, along the trace of a fault between the Dehu and Dehran faults.

A nearby qanat (a water management system consisting of vertical shafts connected by gently sloping tunnels) is apparently offset in a right-lateral sense along the fault trace by ∼13 m (Fig. 4f). The age of this qanat is unknown. Assuming a very approximate age of 800 BC (which is likely to be a maximum age for the introduction of qanat technology to southeast Iran; Magee 2005) this implies a late Holocene slip of ∼5 mm yr^{-1}. Although not impossible, this seems too high, given the estimate derived from the river channel described above, the fact that there is no significant historical or instrumental seismicity record, and that the fault does not perturb the regional GPS-derived velocity field (Vernant *et al*. 2004). It is therefore likely that the qanat offset is not a reliable marker of the fault slip. It may not have originally been a linear feature built across the fault, for example.

Walker *et al*. (2010) found field evidence for young thrust motion across the Jorjafk Fault, in the form of tilted gravel deposits cut by low angle thrusts.

The Rafsanjan Fault lies parallel to and south of the Jorjafk Fault for ∼100 km (Vahdati Daneshmand 1992; Fig. 3). It is mapped as a right-lateral structure (Berberian 1976), but the total offset is not constrained. The western part of the fault zone is notable for the presence of a cluster of Pliocene andesite-dacite volcanoes, lying roughly parallel to the fault (Fig. 6). Eocene volcanics are locally juxtaposed against alluvium, and the fault locally cuts across alluvium (Walker 2006) indicating at least some Quaternary slip. Anticlines to its north deform late Cenozoic strata and may be active structures, overlying blind thrusts. There is no instrumental record of significant seismicity along the fault, but the 1923 September 22 Lalehzar earthquake (29.5°N 56.63°E) was strong enough to kill 200 people, to the southeast of the main fault trace (Walker 2006).

2.3 Anar Fault

The Anar Fault trends NNW–SSE for ∼200 km (Fig. 6). Its right-lateral offset is estimated as ∼25 ± 5 km, based on the displacement of Cretaceous strata in the Kuh-e-Bafq mountains (Walker & Jackson 2004; Meyer & Le Dortz 2007). North of ∼31.5°N the fault zone consists of several strands, which diverge northwards. The Holocene slip rate is estimated at ≥0.8 mm yr^{-1} (Le Dortz *et al*. 2009), based on cosmogenic and optically stimulated luminescence (OSL) dating of offset early Holocene alluvial fan surfaces. No significant earthquakes are recorded from the vicinity of the fault. Two smaller right-lateral faults are present between the Anar and Deh Shir Faults, cutting the Urumieh Dokhtar Zone (Fig. 6). The western fault of the pair displaces a granodiorite stock by ∼2 km (Nabavi 1972).

2.4 Deh Shir Fault

The NNW-SSE Deh Shir (Deshir) Fault is ∼400 km long, much longer than sub-parallel faults to its west and east (Fig. 6). Its structure, offset and possible Holocene slip rate have been described by Walker & Jackson (2004) and Meyer *et al*. (2006) and so are only summarized here. Total right-lateral offset may be as high as 65 ± 15 km, based on displacement of ultramafics from the

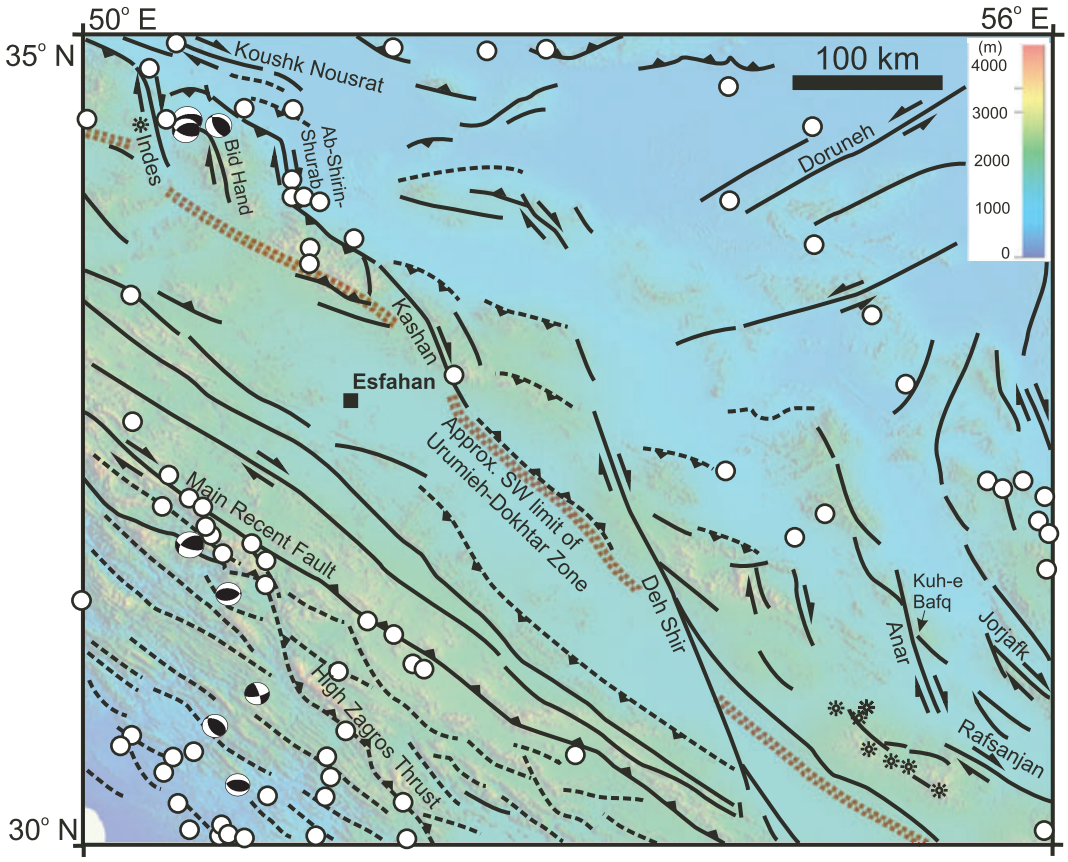

Figure 6. Regional geology of the Anar, Deh Shir, Kashan, Bid Hand, Indes and Qom faults, illustrating their obliquity to the thrusts across the Turkish–Iranian plateau. Thrust locations adapted from Landsat 7 satellite image interpretation and 1:1 000 000 geological maps (NIOC 1977a, 1977b, 1978). Dashed lines indicate blind thrusts, or uncertain locations. Earthquake focal mechanisms are from the Jackson (2001) compilation of body-wave analysed events and from the USGS and Harvard catalogues for events post-2000, filtered for $M_w > 5$ and > 70 per cent double couple. Circles are historical earthquake epicentres from Ambraseys & Melville (1982). Stars indicate volcanic centres, approximately Pliocene in age.

Cretaceous Nain-Baft suture zone (Meyer *et al*. 2006). Volcanics of the Urumieh-Dokhtar Zone are displaced by a similar amount. Most of the fault is a single segment. It is not associated with $M_w > 5$ earthquakes in the instrumental seismicity record, and the historical seismicity record is similarly silent. Displaced rivers and alluvial deposits indicate Holocene slip. This is estimated to be ∼2 mm yr^{-1} by Meyer *et al*. (2006), based on the assumption that offset terrace risers are ∼12 ± 2 ka, that is, early Holocene. This is consistent with the limited age data for similar features in eastern Iran (Fattahi *et al*. 2006; Regard *et al*. 2006), but there are no direct age constraints for the Deh Shir Fault itself. A palaeoseismic study of the fault revealed 1 m deep fissures, with a sandy infill that yielded an OSL age of 2.8 ± 1.4 ka (Nazari *et al*. 2009). This and older fissures and/or colluvial wedges are consistent with events as big as M ∼7 (Nazari *et al*. 2009).

2.5 Kashan (Qom-Zefreh) and Ab-Shirin-Shurab Faults

The Kashan (Qom-Zefreh) Fault consists of a segment parallel to and at the northern margin of the Urumieh-Dokhtar Zone, trending NW–SE, and a NNW–SSE segment that crosses the entire Urumieh-Dokhtar Zone (Fig. 7a; NIOC 1977a, 1977b; Morley *et al*. 2009; Jamali *et al*. 2010). The NW–SE segment is a thrust that puts Eocene volcanic rocks of the Urumieh-Dokhtar Zone against Quaternary alluvial clastics to the northeast. There is a component of right-lateral slip associated with this segment (Jamali *et al*. 2010). The NNW–SSE segment is ∼100 km long and is a sharply defined, linear, right-lateral strike-slip fault. A minimum displacement is given by the offset of the exposed southwestern margin of the Urumieh-Dokhtar Zone: for much of its length across the Turkish–Iranian plateau this belt of mainly Eocene volcanics is linear, with a sharply defined front along the southwestern side (Fig. 7b). The Kashan Fault displaces this volcanic front by at least 40 km (Fig. 7a). This is a minimum estimate. Cretaceous strata lie south of the Eocene volcanics on the west side of the fault, but are not exposed to the east, where Eocene volcanics are the southernmost exposed bedrock before Quaternary alluvium. The actual limit to these volcanics lies an unknown distance south of their exposed limit. Sub-parallel, linear faults lie to both the east and west of the main fault, with presumed but unconstrained right-lateral slip (Fig. 7a). Thrusts define range boundaries north and south of the main outcrop belt; both blind and emergent structures are present (NIOC 1977a). The highest topographic peaks occur close to the intersection of these thrusts and the Kashan Fault, with summits at ∼3500 m and relief of ∼2 km above the plains to the north.

No earthquakes with $M_w > 5$ are recorded from the vicinity of the Kashan Fault in the instrumental record, but an earthquake of estimated M 5.7 took place near the southern tip of the fault in 1344 (Ambraseys & Melville 1982). For most of its trace the Kashan Fault juxtaposes different bedrock lithologies with each other. There are limited extents where bedrock is juxtaposed against alluvium, for example at the extreme southern limit of the fault trace (Fig. 7c).

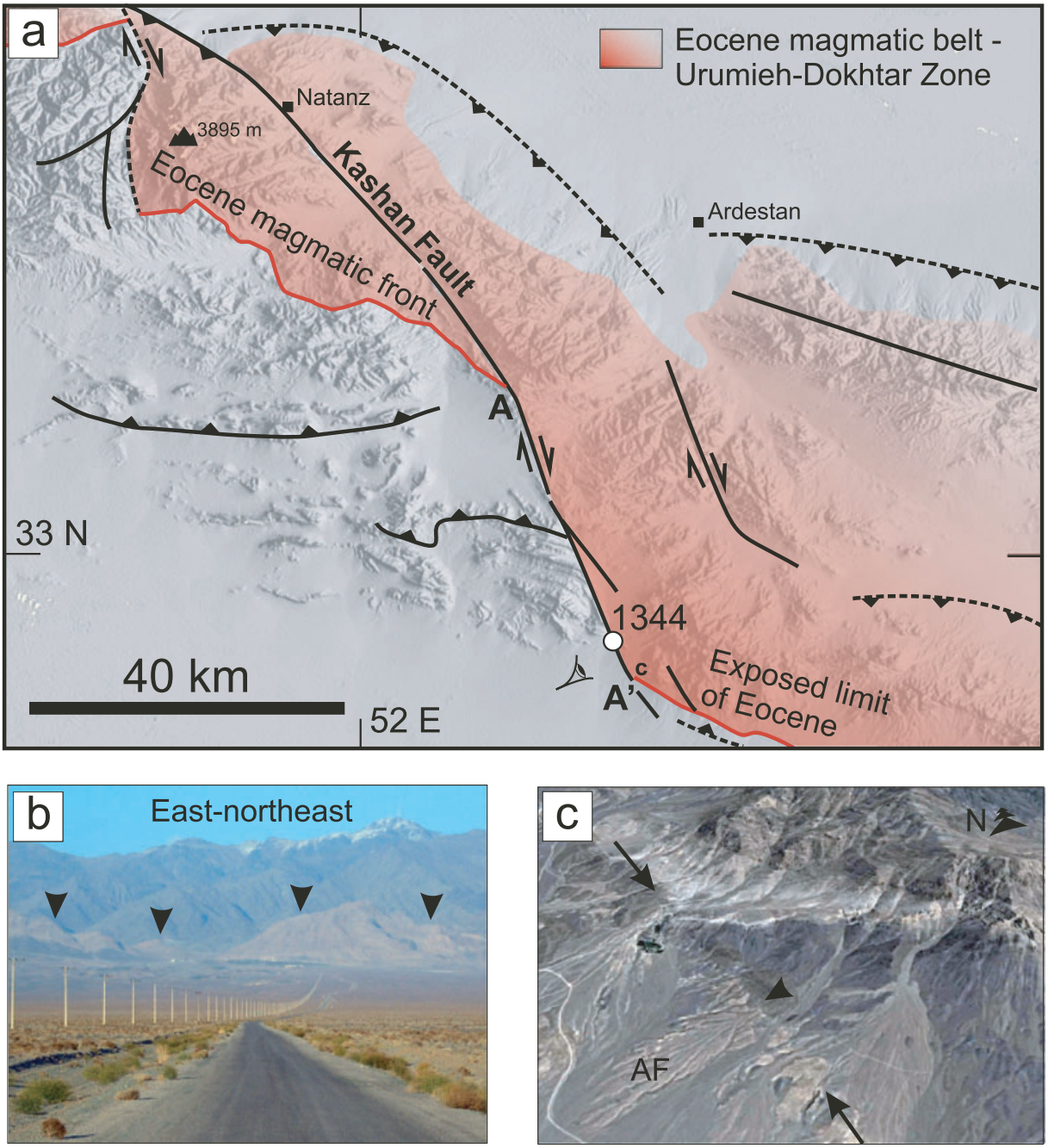

Figure 7. Simplified geology of the Kashan Fault. (a) The southern limit of the Eocene magmatic belt is offset by at least 40 km between piercing points A and A′ (NIOC 1977a). No instrumentally recorded earthquakes with $M_w > 5$ are recorded from this region, but the white circle is the approximate epicentre of an event in 1344 (Ambraseys & Melville 1982). (b) Field photograph of the southeastern section of the Kashan Fault. Arrows highlight the sharp fault trace juxtaposing Mesozoic strata (front) from Eocene volcanics (behind). The 'eye' symbol in (a) shows the approximate viewpoint. (c) Oblique Quickbird image (from Google Earth, ©2010 Google, ©2010 DigitalGlobe) of the southeastern section of the Kashan Fault, showing disrupted alluvial fans along the fault trace (arrowed). The single arrowhead highlights an alluvial fanhead (AF) displaced from upstream drainage. The nearest channel occurs ∼100 m away. The location is marked by the asterisk on (a).

Holocene offset has been detected along the northern part of the fault (Jamali *et al*. 2010), with offset qanats at 33.76°N 51.51°E interpreted to show a minimum Holocene slip rate of 2 mm yr^{-1}. As with the Jorjafk Fault example noted above, offsets derived in this way need to be treated with caution.

At the western end of the NW–SE segment of the Kashan Fault the range front turns in to a NNW–SSE trend, mapped as the Ab-Shirin-Shurab Fault (Fig. 6; Morley *et al*. 2009). This structure offsets Oligo-Miocene strata right-laterally by ∼4 km, close to a point where the range front turns back to a NW–SE trend, and Eocene volcanics and Oligo-Miocene strata are thrust to the north-east (see fig. 26 of Morley *et al*. 2009). Prominent anticlines deform the strata within the basin to the north (Morley *et al*. 2009). This pattern of NNW–SSE strike-slip faults and NW–SE thrusts is strongly developed at least as far as the Indes Fault to the northwest (Fig. 6).

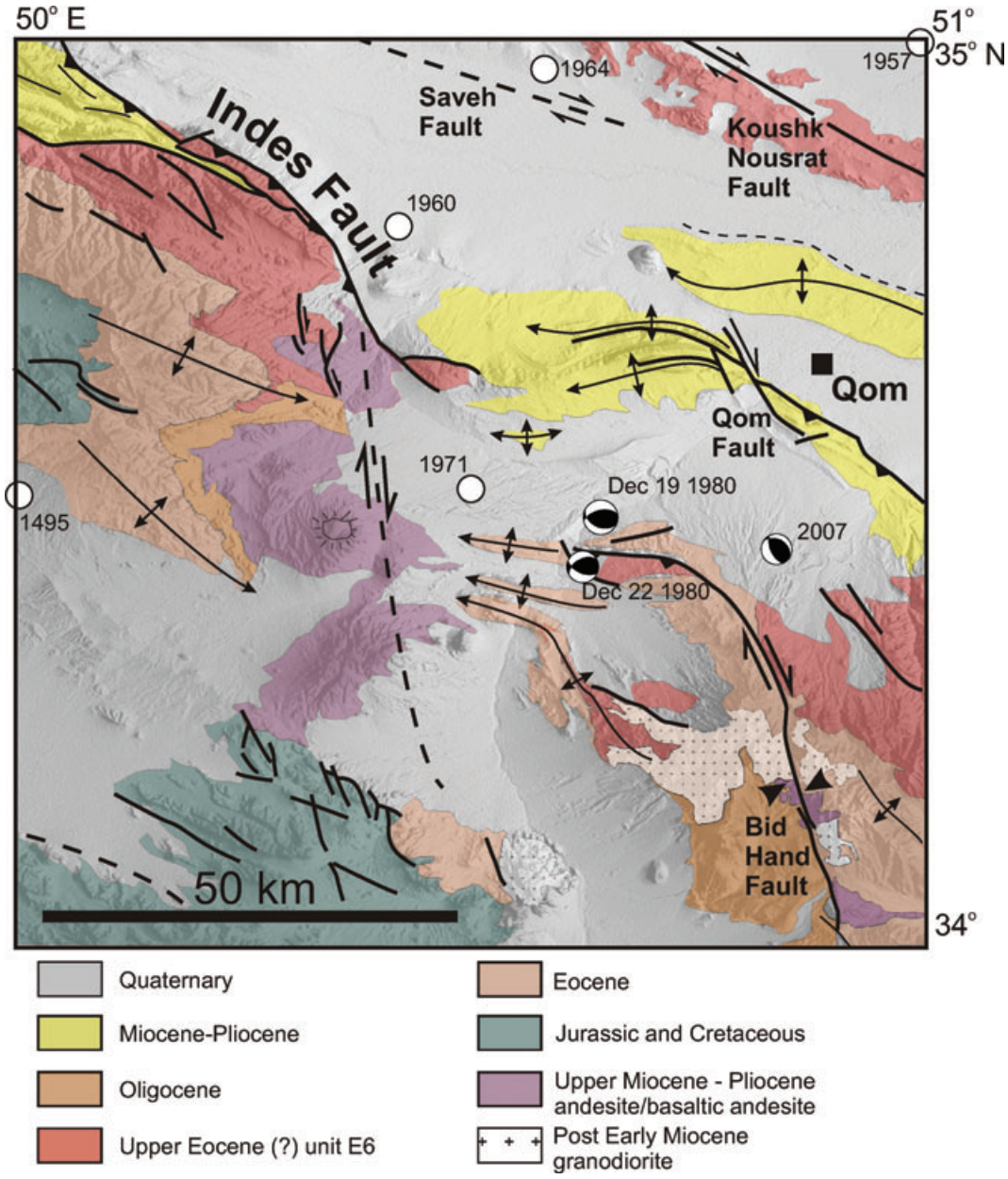

Figure 8. Geology of the Bid Hand, Qom and Indes faults, draped over shaded relief SRTM digital topography. Geology derived from Emami (1981) and Morley *et al*. (2009). Focal mechanisms for the 1980 events are from Priestley *et al*. (1994); the 2007 event is from the Harvard catalogue. Historical epicentres are from Ambraseys & Melville (1982). Solid arrows show piercing points at the northern side of Pliocene lavas along the Bid Hand Fault.

2.6 Bid Hand Fault

The Bid Hand Fault lies south of Qom city, and trends NNW–SSE for 50 km through the Urumieh-Dokhtar Zone (Figs 6 and 8; Emami 1981). The fault is linear and cuts bedrock along the entire length. We have not detected late Quaternary offsets in the geomorphology. Its maximum discernible right-lateral displacement is low: Pliocene basic-intermediate volcanics appear to be offset by $\leq$2 km (Emami 1981; Fig. 8). No offset can be clearly quantified in older lithologies cut by the fault. The southern limit of a granodiorite-syenite intrusion is separated by $\sim$10 km on either side of the fault. However, restoring 10 km of fault slip removes the rough alignment of more northern outcrops of this intrusion. As the granodiorite-syenite intrusion post-dates lower Miocene Qom Formation limestones, the initial faulting is constrained as post Early Miocene or possibly late Early Miocene.

The Bid Hand Fault transfers in the north into a series of folded and thrust Eocene volcanics and Tertiary strata, that trend roughly east–west—that is, anticlockwise of the main NW–SE trend of the Urumieh-Dokhtar Zone (Fig. 8). These folds include the Upper Miocene Upper Red Formation. The southern end of the Bid Hand Fault clips the western side of another Pliocene volcanic field, with no appreciable offset. The fault passes in to a zone of folds and thrusts, within Eocene volcanics. Two earthquakes occurred in 1980 December at the northern end of the Bid Hand Fault (Priestley *et al*. 1994), and show oblique thrusting (Fig. 8). It is not certain which focal plane represents the real fault plane for each event, although a

right-lateral component on a steep south-dipping fault best matches the exposed bedrock geology in the area of the epicentres. A third thrust, on 2007 June 18, occurred further east, and has a more NW–SE strike, in keeping with the local orientation of the Bid Hand Fault in this area (Fig. 8).

2.7 Qom, Saveh and Koushk Nousrat Faults

Tertiary strata, including Upper Miocene marls, are tightly folded and thrust west of Qom city (Zamani-pedram & Hossaini 1998; Figs 6 and 8). Conglomeratic strata mapped as Pliocene (Hezardarreh Formation) lie unconformably above the folds, although they are in places also tilted. Several NNW–SSE right-lateral faults cut across these folds and thrusts (Fig. 8). The Qom (Shad Gholi) Fault is ∼10 km long and offsets folded strata by ∼5 km. The restoration is necessarily approximate because the fold geometry does not match up simply across the fault: fold vergence and thrust dip direction reverse across the strike-slip faults, perhaps indicating that folding/thrusting and strike-slip faulting were at least in part synchronous. Smaller, parallel right-lateral faults occur for up to 10 km further west, with right-lateral offsets up to ∼500 m. There are no instrumentally recorded earthquakes with $M_w > 5$ that are definitely associated with the fault, and no large historical events in the immediate vicinity (Fig. 8). The Saveh and Koushk Nousrat faults lie ∼30 km north of the Qom Fault, and trend NW–SE for ∼90 and ∼130 km, respectively (Figs 1 and 8; Morley *et al*. 2009). The Koushk Nousrat Fault has a right-lateral slip estimated at 9 ± 2 km from an offset fold in Eocene volcanics (Morley *et al*. 2009). There are no estimates for the offset of the Saveh Fault. Earthquakes occurred within 20 km of these faults in 1957 and 1964 (Ambraseys & Melville 1982).

2.8 Indes Fault

The Indes Fault lies west of Qom city (Figs 6 and 8). It cuts through the Eocene magmatic rocks of the NW–SE trending Urumieh-Dokhtar Zone. The same name is used for a fault mapped as a southwest-dipping thrust along the northern outcrop limit and a NNW–SSE segment that lies along the edge of a re-entrant in the range front, that is, where the otherwise linear mountain front steps to the south (Emami 1981; Morley *et al*. 2009). In this latter area Eocene volcanics are juxtaposed with Quaternary alluvium (Fig. 8) along a linear, abrupt topographic step. Further south, the fault trace is covered by Quaternary alluvium or Pliocene volcanics (see later).

The overall slip on the NNW–SSE segment is right lateral: numerous minor faults, parallel to the main zone, have offsets ranging from tens of metres to several kilometres. These faults occur across a width of 20 km. The right-lateral offset of the range front is ∼40 km. This is similar to the offset of the southern outcrop limit of a volcanic unit mapped on both sides of the fault zone ('E6'), forming the uppermost unit of the thick Eocene volcanics in the Urumieh-Dokhtar zone (Fig. 8). We therefore infer that the total right-lateral offset of the main Indes Fault is ∼40 km, with an additional ∼10 km of offset on the sub-parallel faults nearby, giving a total of ∼50 km.

Offset lithologies include basic volcanics mapped as Pliocene (Emami 1981), although the offsets are minor, and overall the volcanics lie across the fault zone as though they post-date the bulk of the offset described above, but are located in a fault-controlled setting. Erosion has exposed dykes that presumably fed the lava flows. These are predominantly oriented north–south, consistent with sigma-3 oriented east–west during the magmatism, that is, east–west extension. Pre-Pliocene rocks on either side of the fault zone are folded in NW–SE trending anticlines that terminate and plunge towards the line of the Indes Fault. This pattern suggests that the folding took place at the same time as at least part of the slip on the Indes Fault, similar to the coeval thrusting and strike-slip faulting taking place within the Zagros at the present time (Authemayou *et al*. 2006).

Earthquakes with estimated magnitude >5 have occurred in the region of the Indes Fault in historical times, in 1495, 1960 and 1971 (Ambraseys & Melville 1982; Fig. 8).

2.9 Soltanieh Fault

The Soltanieh range trends at ∼300°, parallel to and south of the western Alborz mountains in NW Iran (Stöcklin & Eftekharnezhad 1969). Elevations reach over 2500 m. Range-parallel thrusts mark the northern and southern margins of a linear ridge, which exposes rocks of Cambrian to Tertiary age (Figs 9a and b). The Soltanieh Fault lies on the northeastern side of the range, and for most of its 150 km length is mapped as a southwest-dipping thrust, with sub-vertical segments (Berberian 1976). At 36.22° N 49.03°E the fault changes to a NW–SE trend and cuts obliquely across the range interior (Fig. 9). Drainage exploits the fault to cross the Soltanieh range at this point—the only place along the range where drainage crosses the mountains. A syncline of Lower Palaeozoic strata is apparently displaced right-laterally ∼10 km across this segment (Fig. 9a), which in the field consists of both west-dipping and sub-vertical fault strands in a zone ∼1 km across. Fault-bound blocks and lenses of Cambrian carbonate are entrained within Eocene volcanics and volcaniclastic sediments of the Karaj Formation; fault-bound slivers of Jurassic strata are tilted into a vertical orientation (Fig. 9c). There are three minor faults ∼20 km to the southeast, that individually have right-lateral offsets on the kilometre scale (Bolourchi 1969). Collectively, the mapped right-lateral offset is ∼15 km within the Soltanieh range. No instrumentally recorded earthquakes with $M_w > 5$ are recorded from this region, but thrust events occurred to the south in 1962 and 2002 (Fig. 1). There is no clear geomorphic evidence for active deformation.

2.10 North Zanjan Fault

WNW–ESE trending folds and thrusts dominate the structure of the southwestern Alborz mountains, but terminate along a NNW–SSE line, north of the city of Zanjan (Fig. 10a; Stöcklin & Eftekharnezhad 1969). Alluvial sediments occur west of the topographic front. This line is marked as a sub-surface right-lateral fault on the 1:1 000 000 geological map (NIOC 1978), although not on the 1:250 000 sheet (Stöcklin & Eftekharnezhad 1969). We suggest that it is one of the fault set described in this paper. There are no firm offset constraints. The NIOC (1978) map shows a NW–SE sub-surface fault to the southeast, which is offset by 5 km, although there are no offset markers clearly exposed in the geology or geomorphology. We informally call this NNW–SSE structure the North Zanjan Fault.

A prominent west-facing topographic step in the Quaternary alluvial deposits occurs near the intersection of the NW- and NNW-striking range fronts (Figs 10a–b); this lies along the continuation of the supposed fault trace further north. It has a height of ∼25 ± 5 m (Fig. 10c), and trends orthogonal to the rivers coming from the mountains to the east and oblique to the main valley floor to

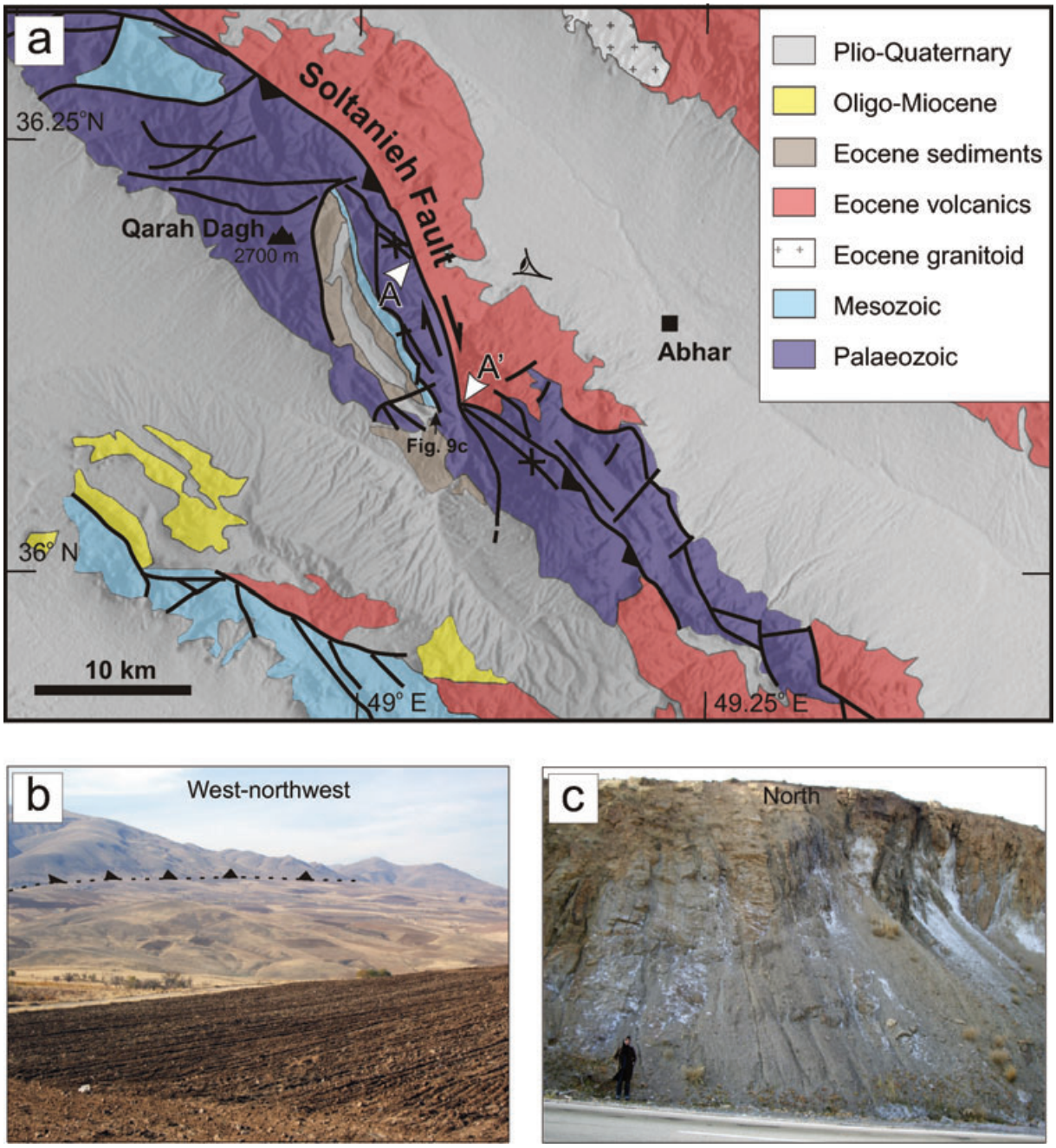

Figure 9. Geology of the Soltanieh Fault in the Abhar region, draped over SRTM digital topography. (a) Derived from the 1:250 000 geological maps of the Zanjan region (Stöcklin & Eftekharnezhad 1969) and Kabudar Ahang region (Bolourchi 1969). An offset syncline from A–A' defines ∼10 km right-lateral slip along the Soltanieh Fault in this area. No instrumentally recorded earthquakes with $M_w > 5$ are recorded from this region, nor does the area have a notable historical seismicity record (Ambraseys & Melville 1982). (b) Field photograph of the Soltanieh Fault west of Abhar, where it overthrusts to the northeast. The 'eye' symbol in (a) shows the approximate viewpoint. (c) Sub-vertical and sheared Jurassic sediments (Shemshak Formation) on the west side of the strike-slip segment of the Soltanieh Fault.

the south: it has the wrong location and orientation to be a terrace related to drainage features. The southern limit of this scarp occurs at the north side of the Zanjan River, which jogs right by ∼1 km at this point (Fig. 10a). The scarp provides geomorphic evidence for late Quaternary activity along the North Zanjan Fault, without confirming that it is an active structure. However, gravel quarries along this scarp at 36.73°N 48.43°E expose thrusts that dip gently east, confirming an element of top-to-west displacement (Figs 10d and e). The river that crosses the scarp at this point jogs right by ∼400 m, although other rivers and streams in the area pass across the fault without lateral displacement. Therefore we conclude that the North Zanjan Fault has evidence for late Quaternary activity, definitely with a thrust component, and probably with a right-lateral component. The total slip and slip rate are unconstrained. There are no instrumentally recorded earthquakes with $M_w > 5$ in the region, and no significant historical record, but the geomorphology described above indicates that it poses significant seismic hazard to the city of Zanjan.

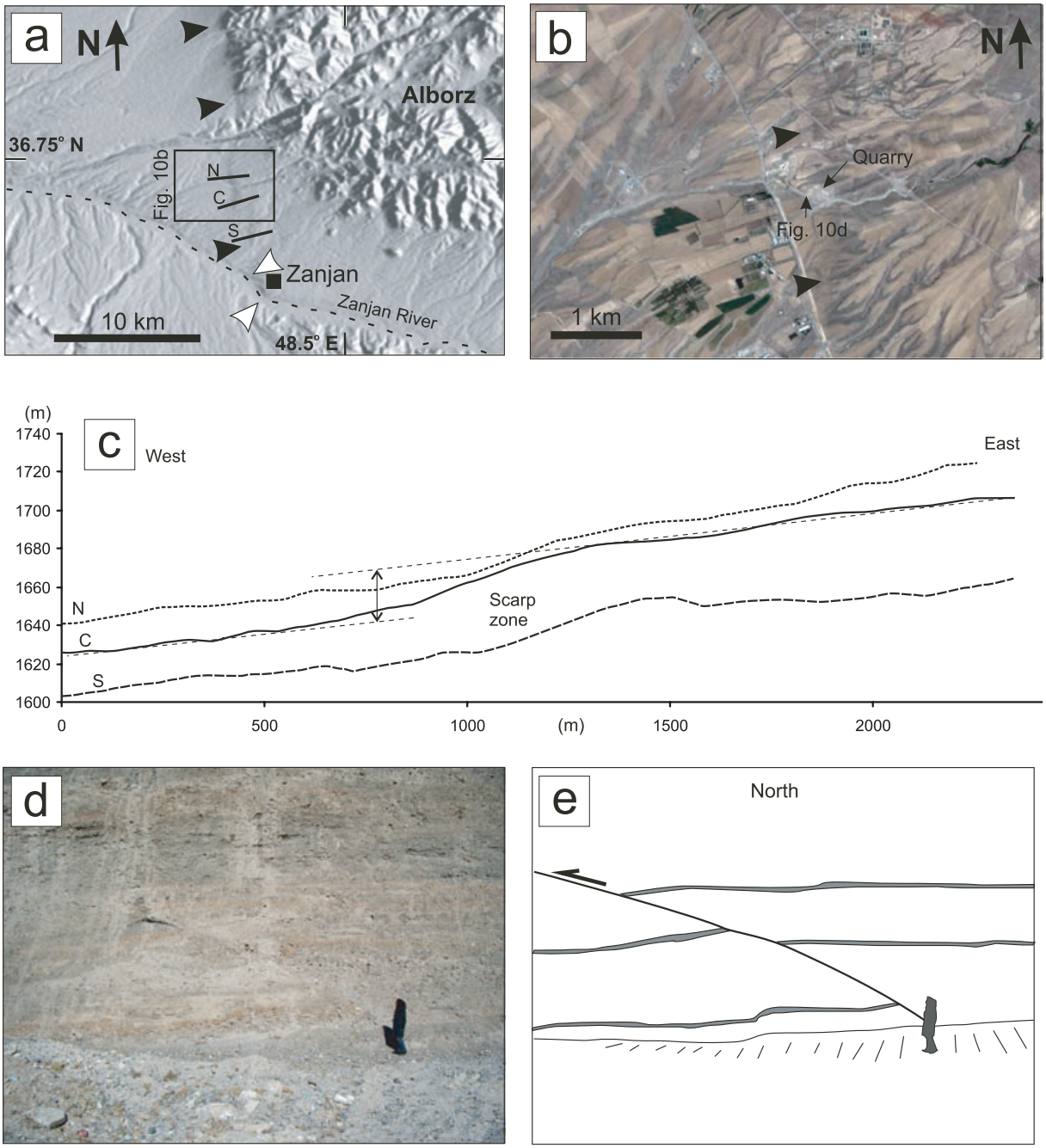

Figure 10. Quaternary faulting in the Zanjan region. (a) SRTM image of abrupt topographic fronts at the southwestern corner of the Alborz mountains. The NNW trending range front (black arrows) is interpreted as a right-lateral oblique-slip thrust, the North Zanjan Fault. White arrows show the right-lateral jog in the course of the Zanjan River. There are no magnitude >5 earthquakes in this region in either the instrumental or historical datasets. (b) Quickbird image (from Google Earth, ©2010 Google, ©2010 DigitalGlobe) of the topographic scarp (arrowed), interpreted as the location of the North Zanjan Fault. (c) Three topographic profiles (N,C,S) across the scarp highlighted in (b), including a reconstruction of the scarp height for the central profile. (d) Field photograph of a thrust in late Quaternary gravel, at the quarry highlighted in (b). (e) Interpretation of (d), highlighting reddish palaeosols developed within the gravels, offset by the thrust.

2.11 Takab (Geynardjeh-Chahartagh) Fault

The linear NNW–SSE Takab (Geynardjeh-Chahartagh) Fault is ~80 km long, roughly 300 km WNW of Tehran (Fig. 11a). It is conventionally mapped as west-directed thrust, placing the Angouran block westwards over the Takab Basin (Alavi & Amidi 1976; Daliran 2008). However, there is no consistent older-over-younger relationship across the fault: Lower-Middle Miocene intermediate-acidic pyroclastics and lavas crop out on both sides of the fault trace (Fig. 11a), in places juxtaposed against older rocks on the west side of the fault zone. There is an apparent 15 km right-lateral offset of this volcanic unit, although the precise amount cannot be constrained, because of the uncertain amount of erosion of the original outcrop limits. Miocene strata of the Upper Red Formation to the west of the fault are sub-horizontal or gently tilted: this is not what is expected in the footwall of a major thrust. Outcrops at 36.58°N

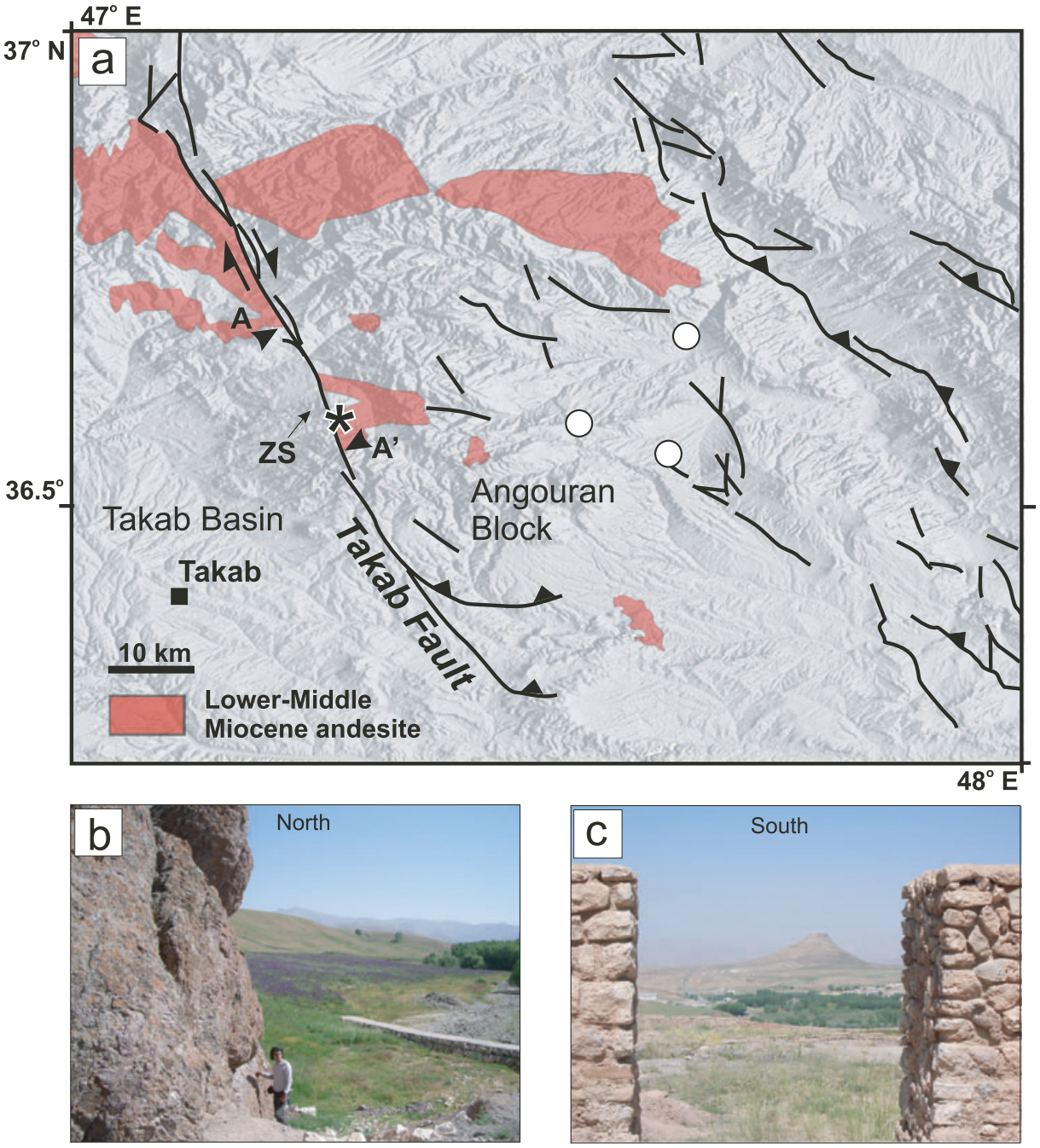

Figure 11. Geology of the Takab (Geynardjeh-Charhartagh) Fault (Alavi & Amidi 1976; Daliran 2008). (a) Topography (SRTM) and extent of the apparent offset of Lower-Middle Miocene volcanics from A-A′. White circles are epicentres of historical earthquakes with estimated magnitude of ≥5 (Ambraseys & Melville 1982). ZS, Quaternary travertine deposits of Zendan-e Soleyman ('Prison of Solomon'). (b) Field photograph of a vertical wall of fault Breccia along the Takab Fault at the starred locality in (a). (c) Field photograph of the travertine mound of Zendan-e Soleyman, adjacent to the Takab Fault (location shown on Fig. 11a). Photograph taken from the walls of the Takht-e Soleyman fortification.

47.27°E reveal that the fault zone is steep to sub-vertical at this locality. Both horizontal and vertical slickenlines are present in fault breccias (Fig. 11b). The southeast end of the fault turns in to a series of east–west trending thrusts.

There is no instrumental record of significant seismicity along the Takab Fault, although three earthquakes with estimated magnitude ≥5 have occurred in the last 130 yr, 30–50 km to its east (Ambraseys & Melville 1982). There are active hydrothermal springs near the fault, and numerous travertine deposits, including the centre of the Takht-e Soleyman UNESCO World Heritage site and the cone of Zendan-e Soleyman (Fig. 11c). The fault does not cut alluvium, or juxtapose bedrock and alluvium along sharp fronts that could be active. Overall, the geology and geomorphology of the fault zone is consistent with a right-lateral oblique thrust, with a strike-slip offset in the order of 15 km, but no evidence for significant late Quaternary activity.

3 KINEMATICS OF DEFORMATION ACROSS CENTRAL IRAN

Previous sections described individual right-lateral faults within the Iranian part of the Turkish–Iranian plateau, north of the Zagros suture (Central Iran), including total offset estimates (Table 1). This section uses these results to address the regional tectonics, and the way(s) such faulting could have contributed to the overall north–south convergence between Arabia and Eurasia (Fig. 12). There is a caveat in that the offset estimates vary in robustness. Also, it is rare that the maximum observed offset affects rocks younger than Eocene: therefore rates of deformation are poorly constrained. What is clear is that the faulting must help accommodate the Arabia–Eurasia convergence. At least three kinematic roles are possible for the faults described, which are not mutually exclusive. Two have been previously proposed for deformation in eastern Iran (Walker & Jackson 2004; Meyer *et al*. 2006).

3.1 Vertical axis block rotations

North–south shortening across Iran could be achieved by the described strike-slip faults if the faults and the blocks they bound rotate anticlockwise about vertical axes (Fig. 12a), similar to the pattern described in the Kopeh Dagh by Hollingsworth *et al*. (2006). There are no palaeomagnetic data to confirm this, but fold axes at the terminations of the strike-slip faults are up to ∼25° anticlockwise of regional trends in several of the fault systems (Fig. 8). The folds may have formed in their present orientations, or there may have been ≤ ∼25° anticlockwise rotation. We do not attempt to apply the geometric method of Hollingsworth *et al*. (2006) to the Central Iranian faults: the variations in the lengths, offsets and fault block widths are too great for an estimate to be derived with any confidence. Another consequence of the strike-slip offsets and vertical axis rotations is that the Central Iran crust should have lengthened along the strike of the collision zone, analogous to the active situation in the Zagros to the south (Talebian & Jackson 2004).

As an aside, we note the presence of left-lateral NE–SW strike-slip faults across much of NE Iran, for example, the Doruneh Fault (Figs 1 and 6; Fattahi *et al*. 2007). These faults have a similarly sparse seismic record as their right-lateral counterparts described in this paper. These are not the focus of our study, but also must play a role in accommodating plate convergence. While some of them may act to transport South Caspian basement westwards (Hollingsworth *et al*. 2008), this is an unlikely explanation for faults as far in to the interior of Iran as Doruneh. Possibly, they act as a rotating array, as discussed above for the right-lateral faults further south (Fig. 12b). This implies the two fault sets rotate with clockwise and anticlockwise senses, in the manner of the fault blocks on the west and east sides of the Aegean (Taymaz *et al*. 1991).

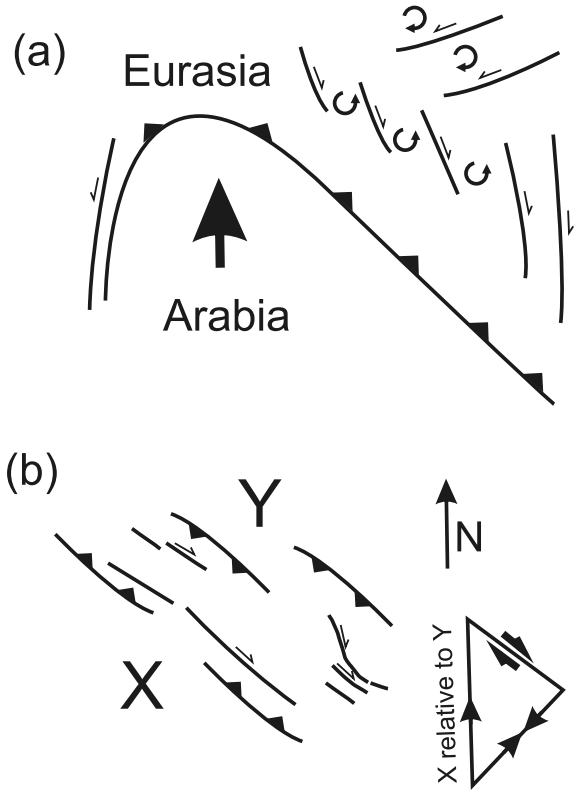

Figure 12. Kinematic summary of the possible roles of right-lateral faulting across Iran. (a) Indentation of Arabian plate northwards achieved on NNW–SSE right-lateral strike-slip faults. Note the presence of left-lateral faults further north. Both fault sets may also undergo vertical rotations, as described in the text, leading to along-strike lengthening of the collision zone. (b) Strain partitioning of north–south convergence via NE–SW shortening on NW–SE thrusts combined with right-lateral strike-slip on NW–SE trending faults.

3.2 Indentation

NNW–SSE strike-slip faults in eastern Iran (Deh Shir, Anar) have previously been suggested as permitting crustal blocks in Iran to move northwards with respect to the crust further east, ultimately the stable Afghan crust at the margin of the collision zone (Meyer *et al*. 2006; Masson *et al*. 2007). This is similar to the purpose suggested for the north–south strike-slip faults in this region (Nayband, Gowk, Neh and Zahedan; Walker & Jackson 2004), and other NNW–SSE or NW–SE faults in this area (e.g. Jorjafk, Kuh Banan) might have a similar function. Work continues on the Quaternary, Holocene and decadal slip rates of these faults, to understand how they accumulate to produce the ∼16 mm yr^{-1} of right-lateral north–south slip observed in the GPS data (Vernant *et al*. 2004). Faults further west lie well within the collision zone, such that it is hard to imagine them acting as part of the eastern boundary system. However, it is possible that the strike-slip faults in eastern Iran collectively allow the Arabian promontory to impinge northwards in to the Eurasian crust (Fig. 12a). Such a mechanism cannot be significant now, given that the bulk of the Arabia–Eurasia convergence across Iran happens north and south of the plateau (Fig. 2a), but is possible for earlier times.

3.3 Thrust and strike-slip division of convergence ('strain partitioning')

Strike-slip at a high angle to the plate convergence vector can have another role in accommodating the overall convergence, where strain is separated in to compressional and strike-slip components ('strain partitioning'). Range-parallel strike-slip and thrust faults in the Zagros and Alborz work together in this way, and it has been possible to combine the total strike-slip and shortening components across the Zagros to calculate the overall north-south convergence across the range (Talebian & Jackson 2002).

Neither the crustal shortening nor the overall north–south convergence across Central Iran is known (north–south convergence

is implied by the plate convergence history, for example, McQuarrie *et al*. 2003). Thrusted range boundaries are commonly NW–SE (Fig. 6), implying NE–SW shortening, that is, at roughly 45° to the overall plate convergence (Morley *et al*. 2009), and therefore in the wrong orientation to accommodate north–south plate convergence on their own. We suggest that the NW–SE trending right-lateral faults across Central Iran contributed to overall plate convergence via strain partitioning, similar to the range-parallel strike-slip faults in the Zagros or Alborz (Fig. 12b). The offset on the main NW–SE strike-slip faults (e.g. Rafsanjan, Jorjafk, Saveh and Koushk Nousrat) is not well constrained, however. Morley *et al*. (2009) estimated as much as 50 km ∼NE–SW shortening across the Central Basin (Fig. 1c), using balanced sections interpreted from seismic data. This suggests 70 km of north–south convergence, if strain partitioning acted as described above.

More plate convergence has taken place within the Sanandaj-Sirjan Zone to the southwest, which contains some of the thickest crust and lithosphere within the whole collision zone (Paul *et al*. 2006; Priestley & McKenzie 2006). Given that major faults within these regions also predominantly trend NW–SE and are a combination of thrusts and strike-slip shear zones (e.g. Sarkarinejad *et al*. 2008), strain partitioning seems likely in these regions too. Strain partitioning is also a possible explanation for the NE–SW left-lateral faults observed in NE Iran (Figs 1 and 6), although we have no detailed constraints.

4 KINEMATIC CHANGE WITHIN THE COLLISION ZONE

The timing of the right-lateral strike-slip deformation across Central Iran is not well constrained, but there is little evidence for rapid, active motion on any of the faults between 48°E and 57°E: they do not perturb the velocity field for Iran by more than 2 mm yr^{-1} (Vernant *et al*. 2004), and seismicity is absent or sporadic compared with active strike-slip faults in the Zagros, for example (Authemayou *et al*. 2006). Similarly, there is little evidence that thrusting is widespread or rapid within Central Iran (Morley *et al*. 2009). Numerous Tertiary stratigraphic units are cut by the strike-slip faults, and provide offset markers, especially the widespread Eocene volcanics but also Miocene formations. It follows that both compressional and strike-slip deformation was active in the Tertiary across Central Iran, but has since slowed or ceased. So, the question follows, why did deformation rates in Central Iran decline in the last few million years (roughly, since ≤5 Ma)? This question ties in with the start or acceleration of deformation in other, still active, areas of the collision zone, noted in the Introduction. Part of the explanation is that it is energetically difficult to keep thickening crust because of the associated buoyancy forces that resist further thickening (Allen *et al*. 2004). This is less likely in the east of Iran than the west, given the lower average elevations around the Dasht-e Lut. It is also an incomplete explanation if at least part of the strike-slip faulting achieved convergence via vertical axis rotations, as these do not thicken the crust or lead to increased elevations. Active strike-slip faulting across much of Tibet is an example of such tectonics within the other great orogenic plateau of Asia (Taylor *et al*. 2003).

Another possible explanation lies in the tectonics of the crust east of the present Arabia–Eurasia collision zone (Fig. 13). Although collision of the Indian plate with Eurasia to its north took place in the early Tertiary, collision along the western margin apparently occurred much later, possibly as recently as the Pliocene (Treloar & Izatt 1993). This estimate is based on the age of initial deformation in the Katawaz Basin of Pakistan and its equivalents. Treloar & Izatt (1993) relate this young deformation to the highly oblique, right-lateral shear along the western side of the Indian plate, which eventually brought collision between India and the composite continental crust of south central Asia known as the Afghan block (Fig. 13). Before this collision the Afghan block crust was bordered by oceanic crust to its east, which was effectively a 'free face' in the jargon of escape/extrusion tectonics.

We speculate that before the Afghan–India collision, the crust in Central Iran was able to move laterally to the southeast, as the result of the strike-slip described in this paper, transferring strain into Afghanistan (Fig. 13a). Once Afghan–India collision was underway this mechanism stopped being viable, sometime in the Pliocene (∼5–2 Ma). While strike-slip faulting and crustal thickening within the Turkish–Iranian plateau diminished, the continuing plate convergence had to be achieved in other ways. This includes the folding and thrusting within and around the South Caspian Basin, possibly during westward movement of this block (Hollingsworth *et al*. 2008) and the initiation or acceleration of the western 'escape' of Anatolia (Fig. 13b; McKenzie 1972).

5 CONCLUSIONS

Right-lateral faults across Iran form an array that achieved at least ∼250 km of slip in the Cenozoic, but shows no sign of rapid movement today (Table 1). Eastern faults (Deh Shir, Anar and Kuh Banan) may have Holocene slip rates of ≤2 mm yr^{-1} (Meyer *et al*. 2006) but even these rates are unlikely further west. This is not to say that the faults are inactive; there is evidence from both the geomorphology and historical seismicity records that most faults in this study have had Holocene activity.

Collectively, these faults and the fault blocks they define make a contribution to the overall Arabia–Eurasia convergence through vertical axis rotations, but the magnitude of this is not constrained. Their orientation, scale and slip sense suggest that they performed other roles, namely (1) allowing indentation of Arabia in to Eurasia and (2) acting in concert with NE–SW directed crustal shortening in Central Iran to achieve overall north–south convergence, via strain partitioning.

As neither rapid thrusting nor strike-slip occur within Central Iran today, the question follows why should the regional tectonics have changed in the last few million years? Part of the explanation may lie in the buoyancy force associated with topographically high crust: this resists further shortening via thickening, causing deformation to propagate in to previously undeformed areas in the forelands of the orogen. An alternative, complementary, explanation is that the Afghan–India collision (Treloar & Izatt 1993) prevented the lengthening of Iranian crust in a southeast direction, which was a consequence of the right-lateral strike-slip faulting across Iran. With the 'free face' closed, Arabia–Eurasia convergence began to be accommodated with the present strain pattern (Fig. 13). Intriguingly, this may apply as far as the western end of the collision zone in western Turkey, given that the North Anatolian Fault only requires a few million years at present slip rates (24 ± 1 mm yr^{-1}; McClusky *et al*. 2000) to achieve its total displacement of ∼85 km (Seymen 1975). A change in boundary conditions at one side of the India–Asia collision zone could have influenced deformation as far away as the distant side of the Arabia–Eurasia collision, across ∼4000 km of intervening continental crust.

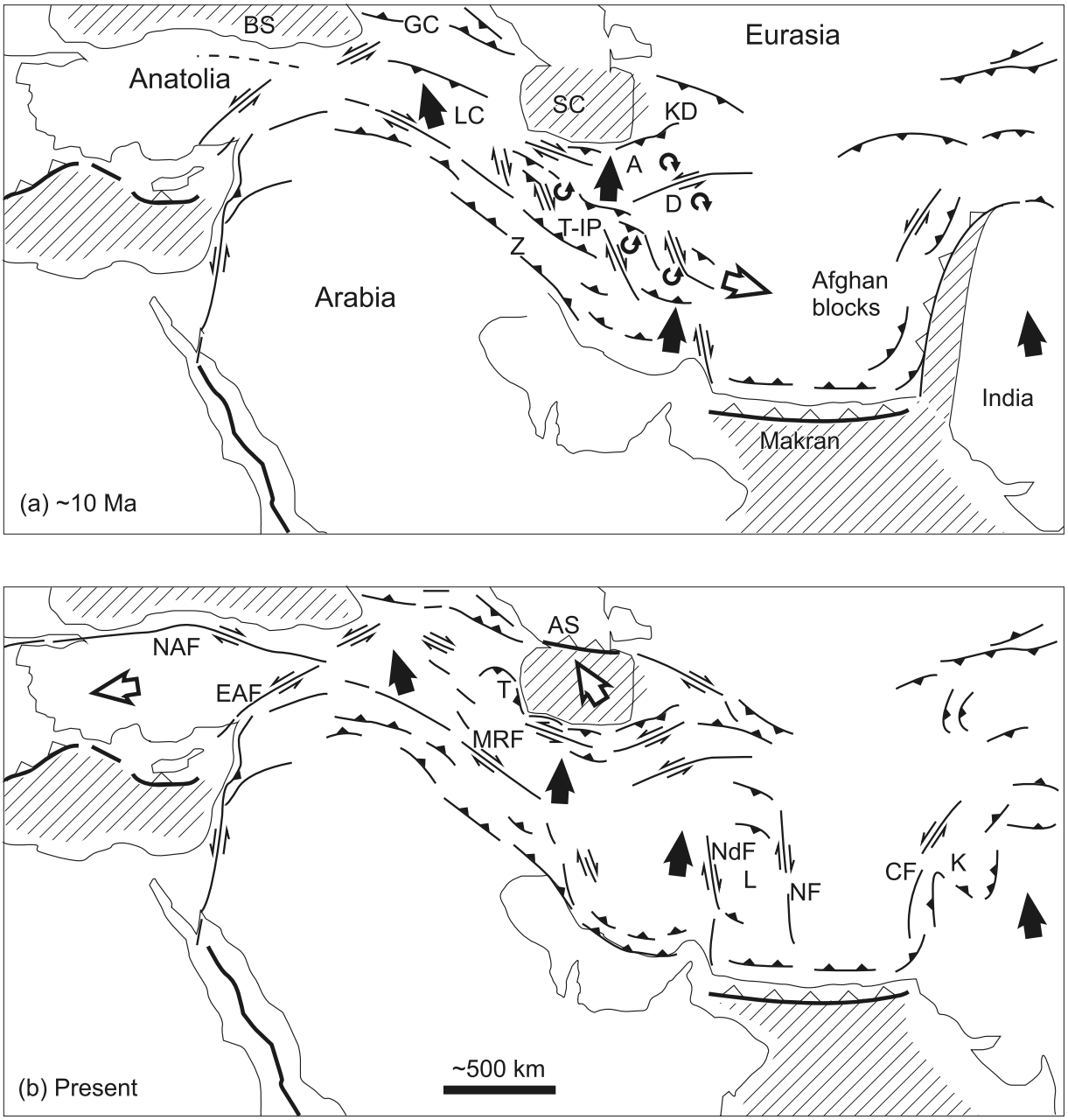

Figure 13. Cartoons for the kinematics of the Arabia–Eurasia collision, before (a) and after (b) the collision of Afghan crust with the western margin of the Indian plate in the Pliocene. Shaded areas are oceanic crust. Solid arrows denote motion within the collision zone with respect to stable Eurasia, adapted for (b) from the GPS-derived velocity field (Vernant *et al*. 2004; Reilinger *et al*. 2006). Open arrows show motion at a high angle to the overall convergence vector, including the inferred elongation of the Turkish–Iranian plateau to the southeast (Fig. 12a). Abbreviations: A, Alborz; AS, Absheron Sill; BS, Black Sea; CF, Chaman Fault; D, Doruneh Fault; EAF, East Anatolian Fault; GC, Greater Caucasus; K, Katawaz Basin; KD, Kopeh Dagh; L, Lut; LC, Lesser Caucasus; MRF, Main Recent Fault; NF, Neh Fault; NAF, North Anatolian Fault; NdF, Nayband Fault; SC, South Caspian Basin; T, Talesh; T-IP, Turkish–Iranian plateau; Z, Zagros.

ACKNOWLEDGMENTS

This work would not have been possible without the help of the Geological Survey of Iran, and we thank Morteza Talebian, Mohammad Ghassemi and Manouchehr Ghorashi for their support. MBA was supported by Durham research project R050471. MBA and MK acknowledge Royal Society support. We thank Richard Walker for discussions on the geology of Iran and Nicholas Ambraseys for access to historical earthquake data. Christine Authemayou and an anonymous referee provided very helpful reviews.

REFERENCES

Agard, P., Omrani, J., Jolivet, L. & Mouthereau, F., 2005. Convergence history across Zagros (Iran): constraints from collisional and earlier deformation, *Int. J. Earth. Sci.,* **94,** 401–419.

Alavi, M. & Amini, M., 1976. Geological Quadrangle map of Iran, 1:250,000 scale, sheet C4 (Takab), Geological Survey of Iran.

Allen, M.B. & Armstrong, H.A., 2008. Arabia-Eurasia collision and the forcing of mid Cenozoic global cooling, *Palaeogeogr., Palaeoclimatol., Palaeoecol.,* **265,** 52–58.

Allen, M.B., Ghassemi, M.R., Shahrabi, M. & Qorashi, M., 2003. Accommodation of late Cenozoic oblique shortening in the Alborz range, northern Iran, *J. Struct. Geol.,* **25,** 659–672.

Allen, M., Jackson, J. & Walker, R., 2004. Late Cenozoic reorganization of the Arabia-Eurasia collision and the comparison of short-term and long-term deformation rates, *Tectonics,* **23,** TC2008, doi:2010.1029/2003TC001530.

Ambraseys, N.N. & Melville, C.P., 1982. *A History of Persian Earthquakes,* Cambridge University Press, Cambridge.

Authemayou, C., Chardon, D., Bellier, O., Malekzadeh, Z., Shabanian, E. & Abbassi, M.R., 2006. Late Cenozoic partitioning of oblique plate convergence in the Zagros fold-and-thrust belt (Iran), *Tectonics,* **25,** TC3002, doi:10.1029/2005tc001860.

Ballato, P., Uba, C.E., Landgraf, A., Strecker, M.R., Sudo, M., Stockli, D.F., Friedrich, A. & Tabatabaei, S.H., 2010. Arabia-Eurasia continental collision: insights from late Tertiary foreland basin evolution in the Alborz mountains, northern Iran. *Bull. Geol. Soc. Am.*, in press, doi:10.1130/B30091.1.

Berberian, M., 1976. Contribution to the seismotectonics of Iran (part II), Report No. 39, Geological Survey of Iran.

Berberian, M., 1995. Master "blind" thrust faults hidden under the Zagros folds: active basement tectonics and surface morphotectonics, *Tectonophysics,* **241,** 193–224.

Berberian, M. & Yeats, R.S., 1999. Patterns of historical earthquake rupture in the Iranian plateau, *Bull. seism. Soc. Am.,* **89,** 120–139.

Berberian, M., Asudeh, I. & Arshadi, S., 1979. Surface rupture and mechanisms of the Bob-Tangol (southeasern Iran) earthquake of 19 December 1977, *Earth. planet. Sci. Lett.,* **42,** 456–462.

Blanc, E.J.-P., Allen, M.B., Inger, S. & Hassani, H., 2003. Structural styles in the Zagros Simple Folded Zone, Iran, *J. Geol. Soc., London,* **160,** 400–412.

Bolourchi, M.H., 1969. Geological Quadrangle map of Iran, 1:250,000 scale, sheet D5 (Kabudar Ahang), Geological Survey of Iran.

Copley, A. & Jackson, J., 2006. Active tectonics of the Turkish-Iranian Plateau, *Tectonics,* **25,** TC6006, doi:10.1029/2005TC001096.

Daliran, F., 2008. The carbonate rock-hosted epithermal gold deposit of Agdarreh, Takab geothermal field, NW Iran – hydrothermal alteration and mineralisation, *Miner. Depos.,* **43,** 383–404.

Emami, M.H., 1981. Geological Quadrangle map of Iran, 1:250,000 scale, sheet E6 (Qom), Geological Survey of Iran.

Fattahi, M., Walker, R., Hollingsworth, J., Bahroudi, A., Nazari, H., Talebian, M., Armitage, S. & Stokes, S., 2006. Holocene slip-rate on the Sabzevar thrust fault, NE Iran, determined using optically stimulated luminescence (OSL), *Earth. planet. Sci. Lett.,* **245,** 673–684.

Fattahi, M., Walker, R.T., Khatib, M.M., Dolati, A. & Bahroudi, A., 2007. Slip-rate estimate and past earthquakes on the Doruneh fault, eastern Iran, *Geophys. J.Int.,* **168,** 691–709.

Garfunkel, Z., 1981. Internal structure of the Dead Sea leaky transform (rift) in relation to plate kinematics, *Tectonophysics,* **80,** 81–108.

Guest, B., Axen, G.J., Lam, P.S. & Hassanzadeh, J., 2006. Late Cenozoic shortening in the west-central Alborz Mountains, northern Iran, by combined conjugate strike-slip and thin-skinned deformation, *Geosphere,* **2,** 35–52.

Hollingsworth, J., Jackson, J., Walker, R., Gheitanchi, M.R. & Bolourchi, M.J., 2006. Strike-slip faulting, rotation, and along-strike elongation in the Kopeh Dagh mountains, NE Iran, *Geophys. J. Int.,* **166,** 1161–1177.

Hollingsworth, J., Jackson, J., Walker, R. & Nazari, H., 2008. Extrusion tectonics and subduction in the eastern South Caspian region since 10 Ma, *Geology,* **36,** 763–766.

Hollingsworth, J., Fattahi, M., Walker, R., Talebian, M., Bahroudi, A., Bolourchi, M.J., Jackson, J. & Copley, A., 2010. Oroclinal bending, distributed thrust and strike-slip faulting, and the accommodation of Arabia-Eurasia convergence in NE Iran since the Oligocene, *Geophys. J. Int.,* **181,** 1214–1246.

Jackson, J., 2001. Living with earthquakes: know your faults, *J. earthq. Eng.,* **5,** 5–123.

Jackson, J., Haines, A.J. & Holt, W.E., 1995. The accommodation of Arabia-Eurasia plate convergence in Iran, *J. geophys. Res.,* **100,** 15 205–15 209.

Jackson, J., Priestley, K., Allen, M. & Berberian, M., 2002. Active tectonics of the South Caspian Basin, *Geophys. J. Int.,* **148,** 214–245.

Jamali, F., Hessami, K. & Ghorashi, M., 2010. Active tectonics and strain partitioning along dextral fault system in Central Iran: analysis of geomorphological observations and geophysical data in the Kashan region, *J. Asian Earth Sci.*, in press.

Le Dortz, K., *et al*., 2009. Holocene right-slip rate determined by cosmogenic and OSL dating on the Anar fault, Central Iran, *Geophys. J. Int.,* **179,** 700–710.

Magee, P., 2005. The chronology and environmental background of Iron Age settlement in southeastern Iran and the question of the origin of the qanat irrigation system. *Iranica Antiqua,* **40,** 217–231.

Maggi, A. & Priestley, K., 2005. Surface waveform tomography of the Turkish-Iranian plateau, *Geophys. J. Int.,* **160,** 1068–1080.

Mahdavi, M.A., 1996. Geological Quadrangle map of Iran, 1:250,000 scale, sheet NH 40.2 (Ravar), Geological Survey of Iran.

Masson, F., Anvari, M., Djamour, Y., Walpersdorf, A., Tavakoli, F., Daignieres, M., Nankali, H. & Van Gorp, S., 2007. Large-scale velocity field and strain tensor in Iran inferred from GPS measurements: new insight for the present-day deformation pattern within NE Iran, *Geophys. J. Int.,* **170,** 436–440.

McClusky, S., *et al*., 2000. Global Positioning System constraints on plate kinematics and dynamics in the eastern Mediterranean and Caucasus, *J. geophys. Res.,* **105,** 5695–5719.

McKenzie, D.P., 1972. Active tectonics of the Mediterranean region, *Geophys. J. R. astr. Soc.,* **30,** 109–185.

McQuarrie, N., Stock, J.M., Verdel, C., & Wernicke, B., 2003. Cenozoic evolution of Neotethys and implications for the causes of plate motions, *Geophys. Res. Lett.,* **30,** art. no. 2036 doi:2010.1029/2003GL017992.

McQuarrie, N., 2004. Crustal scale geometry of the Zagros fold-thrust belt, Iran, *J. Struct. Geol.,* **26,** 519–535.

Meyer, B. & Le Dortz, K., 2007. Strike-slip kinematics in Central and Eastern Iran: estimating fault slip-rates averaged over the Holocene, *Tectonics,* **26,** TC5009, doi: 10.1029/2006tc002073.

Meyer, B., Mouthereau, F., Lacombe, O. & Agard, P., 2006. Evidence of Quaternary activity along the Deshir Fault: implication for the Tertiary tectonics of central Iran, *Geophys. J. Int.,* **164,** 192–201.

Morley, C.K., *et al*. 2009. Structural development of a major late Cenozoic basin and transpressional belt in central Iran: The Central Basin in the Qom-Saveh area, *Geosphere,* **5,** 325–362.

Nabavi, M.H., 1972. Geological Quadrangle map of Iran, 1:250,000 scale, sheet H9 (Yazd), Geological Survey of Iran.

National Iranian Oil Company, 1977a. Geological Map of Iran, 1:1,000,000 scale, sheet 2 North-Central Iran, National Iranian Oil Company, Tehran.

National Iranian Oil Company, 1977b. Geological Map of Iran, 1:1,000,000 scale, sheet 5 South-Central Iran, National Iranian Oil Company, Tehran.

National Iranian Oil Company, 1978. Geological Map of Iran, 1:1,000,000 scale, sheet 1 North-West Iran, National Iranian Oil Company, Tehran.

Nazari, H., *et al*., 2009. First evidence for large earthquakes on the Deshir Fault, Central Iran Plateau, *Terra Nova,* **21,** 417–426.

Okay, A.I., Zattin, M. & Cavazza, W., 2010. Apatite fission-track data for the Miocene Arabia-Eurasia collision, *Geology,* **38,** 35–38.

Paul, A., Kaviani, A., Hatzfeld, D., Vergne, J. & Mokhtari, M., 2006. Seismological evidence for crustal-scale thrusting in the Zagros mountain belt (Iran), *Geophys. J. Int.,* **166,** 227–237.

Philip, H., Cisternas, A., Gvishiani, A. & Gorshkov, A., 1989. The Caucasus: an actual example of the initial stages of a continental collision, *Tectonophysics,* **161,** 1–21.

Priestley, K., Baker, C. & Jackson, J., 1994. Implications of earthquake focal mechanism data for the active tectonics of the South Caspian Basin and surrounding regions, *Geophys. J. Int.,* **118,** 111–141.

Priestley, K. & McKenzie, D., 2006. The thermal structure of the lithosphere from shear wave velocities, *Earth. planet. Sci. Lett.,* **244,** 285–301.

Regard, V., *et al*., 2006. Be-10 dating of alluvial deposits from Southeastern Iran (the Hormoz Strait area), *Palaeogeogr., Palaeoclimatol., Palaeoecol.,* **242,** 36–53.

Reilinger, R., *et al*., 2006. GPS constraints on continental deformation in the Africa-Arabia-Eurasia continental collision zone and implications

for the dynamics of plate interactions, *J. geophys. Res.,* **111,** B05411, doi:05410.01029/02005JB004051.

Ritz, J.F., Nazari, H., Ghassemi, A., Salamati, R., Shafei, A., Solaymani, S. & Vernant, P., 2006. Active transtension inside central Alborz: a new insight into northern Iran-southern Caspian geodynamics, *Geology,* **34,** 477–480.

Sahandi, M., 1992. Geological Quadrangle map of Iran, 1:250,000 scale, sheet J10 (Kerman), Geological Survey of Iran.

Sarkarinejad, K., Faghih, A. & Grasernann, B., 2008. Transpressional deformations within the Sanandaj-Sirjan metamorphic belt (Zagros Mountains, Iran), *J. Struct. Geol.,* **30,** 818–826.

Seymen, I., 1975. Tectonic characteristics of the North Anatolian Fault zone in the Kelkit Valley segment, *PhD thesis*, Istanbul Teknik Universitesi Maden Fakultesi Yayinlari, Istanbul.

Stöcklin, J. & Eftekharnezhad, J., 1969. Geological Quadrangle map of Iran, 1:250,000 scale, sheet D4 (Zanjan), Geological Survey of Iran.

Talebian, M. & Jackson, J., 2002. Offset on the Main Recent Fault of NW Iran and implications for the late Cenozoic tectonics of the Arabia-Eurasia collision zone, *Geophys. J. Int.,* **150,** 422–439.

Talebian, M. & Jackson, J., 2004. A reappraisal of earthquake focal mechanisms and active shortening in the Zagros mountains of Iran, *Geophys. J. Int.,* **156,** 506–526.

Talebian, M., *et al*., 2006. The Dahuiyeh (Zarand) earthquake of 2005 February 22 in central Iran: reactivation of an intramountain reverse fault, *Geophys. J. Int.,* **164,** 137–148.

Taylor, M., Yin, A., Ryerson, F.J., Kapp, P. & Ding, L., 2003. Conjugate strike-slip faulting along the Bangong-Nujiang suture zone accommodates coeval east-west extension and north-south shortening in the interior of the Tibetan Plateau, *Tectonics,* **22,** TC1044. doi:10.1029/2002tc001361.

Taymaz, T., Jackson, J.A. & McKenzie, D., 1991. Active tectonics of the north and central Aegean Sea, *Geophys. J. Int.,* **106,** 403–490.

Treloar, P.J. & Izatt, C.N., 1993. Tectonics of the Himalayan collision between the Indian Plate and the Afghan Block: a synthesis, *Geol. Soc. Lond. Spec. Pub.,* **74,** 69–87.

Vahdati Daneshmand, F., 1992. Geological Quadrangle map of Iran, 1:250,000 scale, sheet I40 (Rafsanjan), Geological Survey of Iran.

Vernant, P., *et al*., 2004. Contemporary crustal deformation and plate kinematics in Middle East constrained by GPS measurements in Iran and northern Iran, *Geophys. J. Int.,* **157,** 381–398.

Vincent, S.J., Allen, M.B., Ismail-Zadeh, A.D., Flecker, R., Foland, K.A. & Simmons, M.D., 2005. Insights from the Talysh of Azerbaijan into the Paleogene evolution of the South Caspian region, *Bull. geol. Soc. Am.,* **117,** 1513–1533.

Walker, R.T., 2006. A remote sensing study of active folding and faulting in southern Kerman province, SE Iran, *J. Struct. Geol.,* **28,** 654–668.

Walker, R. & Jackson, J., 2004. Active tectonics and late Cenozoic strain distribution in central and eastern Iran, *Tectonics,* **23,** TC5010, doi:5010.1029/2003TC001529.

Walker, R.T., Gans, P., Allen, M.B., Jackson, J., Khatib, M., Marsh, N. & Zarrinkoub, M., 2009. Late Cenozoic volcanism and rates of active faulting in eastern Iran, *Geophys. J. Int.,* **177,** 783–805.

Walker, R.T., Talebian, M., Saiffori, S., Sloan, R.A., Rasheedi, A., MacBean, N. & Ghassemi, A., 2010. Active faulting, earthquakes, and restraining bend development near Kerman city in southeastern Iran, *J. Struct. Geol.,* **32,** 1046–1060, doi:10.1016/j.jsg.2010.06.012.

Westaway, R., 1994. Present-day kinematics of the Middle-East and Eastern Mediterranean, *J. geophys. Res.,* **99,** 12 071–12 090.

Zamami-pedram, M. & Hossaini, H., 1998. Geological Quadrangle map of Iran, 1:100,000 scale, sheet 6159 (Qom), Geological Survey of Iran.